Schizosaccharomyces pombe KAT5 contributes to resection and repair of a DNA double strand break

Tingting Li[1], Ruben C. Petreaca[1&2] and Susan L. Forsburg[1&*]

[1]Program of Molecular and Computational Biology, University of Southern California, Los Angeles CA 90089-2910

[2]Department of Molecular Genetics, Ohio State University, Marion OH 43302

*Corresponding author at Forsburg@usc.edu

Keywords: fission yeast, DSB repair, KAT5, Mst1, resection

Abstract

Chromatin remodeling is essential for effective repair of a DNA double strand break. KAT5 (*S. pombe* Mst1, human TIP60) is a MYST family histone acetyltransferase conserved from yeast to humans that coordinates various DNA damage response activities at a DNA double strand break (DSB), including histone remodeling and activation of the DNA damage checkpoint. In *S. pombe*, mutations in *mst1*$^+$ causes sensitivity to DNA damaging drugs. Here we show that Mst1 is recruited to DSBs. Mutation of *mst1*$^+$ disrupts recruitment of repair proteins and delays resection. These defects are partially rescued by deletion of *pku70*, which has been previously shown to antagonize repair by homologous recombination. These phenotypes of *mst1* are similar to *pht1-4KR*, a non-acetylatable form of histone variant H2A.Z, which has been proposed to affect resection. Our data suggest that Mst1 functions to direct repair of DSBs towards homologous recombination pathways by modulating resection at the double strand break.

Introduction

The DNA damage response choreographs multiple cellular activities such as lesion detection, activation of the DNA damage checkpoint, break repair, and recovery (rev. in (Langerak and Russell 2011)). Chromatin remodeling is central to the faithful execution of these processes, requiring the coordination of histone modifiers, remodelers, and chromatin assembly factors (rev. in (Bakkenist and Kastan 2015; Clouaire and Legube 2019; Aleksandrov *et al.* 2020)). Acetylation of histone H4 is one marker associated with chromatin remodeling at a double strand break (DSB), a potentially lethal form of DNA damage. There is good evidence that histone H4 acetylation is linked to radioresistance and the repair response, possibly by facilitating chromatin mobilization (rev. in (Dhar *et al.* 2017; Van and Santos 2018)).

The MYST family of histone acetyltransferases (HATs) is defined by a distinct catalytic domain, and its members are implicated in histone acetylation at DSBs (rev. in (Utley and Côté 2003; Thomas and Voss 2007)). KAT5 is the most highly conserved HAT of this family, known as Mst1 in *S. pombe,* Esa1 in *S.*

cerevisiae, and TIP60 in mammals (rev. in (Avvakumov and Côté 2007; Pillus 2008)). The gene is essential for viability in all species, because in addition to its role in DSB repair it performs other functions such as transcriptional regulation, heterochromatin assembly and centromere assembly (rev. in (Pillus 2008)). In humans, TIP60 has also been identified as a tumor suppressor (rev. in (Sapountzi *et al.* 2006; Voss and Thomas 2009) and is a therapeutic target (rev. in (Judes *et al.* 2015)).

KAT5 contains a chromodomain in addition to its HAT domain, which suggests that it binds methylated histones (rev. in (Utley and Côté 2003; De La Cruz *et al.* 2005)). KAT5 functions in the context of a large protein complex called NuA4, and acetylates numerous substrates including histones H2A, H3, and H4, and the histone variants H2A.X and H2A.Z (Kimura and Horikoshi 1998; Smith *et al.* 1998; Allard *et al.* 1999; Galarneau *et al.* 2000; Babiarz *et al.* 2006; Keogh *et al.* 2006). Evidence from human cells has shown that KAT5 can acetylate non-histone proteins as well, including the checkpoint kinase ATM and the tumor suppressor TP53 (Sun *et al.* 2005; Jiang *et al.* 2006; Leduc *et al.* 2006; Sykes *et al.* 2006; Tang *et al.* 2006; Kim *et al.* 2007; Naidu *et al.* 2012; Ortega-Atienza *et al.* 2016). Importantly, NuA4 cooperates with the Swr1 chromatin remodeler that is required for exchange of histone H2A with the variant H2A.Z ((rev. in (Scacchetti and Becker 2021) (Kobor *et al.* 2004; Krogan *et al.* 2004; Keogh *et al.* 2006; Zhou *et al.* 2010)).

Evidence from both yeast and humans shows that the NuA4 complex is recruited to DSBs by multiple binding partners including phosphorylated H2A(X) (Downs *et al.* 2004), methylated histone H4K20 (Jacquet *et al.* 2016), methylated histone H3K36 (Li and Wang 2017), methylated histone H3K9 via the KAT5 chromodomain (Sun et al. 2005; Sun et al. 2009, Ayrapetov et al. 2014), and interaction with Nbs1, a component of the end-binding resection complex MRN (Cheng *et al.* 2018). In fission yeast, physical association between KAT5/SpMst1 and the homologous recombination protein Rad52 has also been demonstrated (Gómez *et al.* 2008). However, how these recruiting partners cooperate or compete with each other is unknown.

Recruitment of the NuA4 complex to the sites of DSBs has several outcomes. There is evidence that the recruitment of variant H2A.Z and its subsequent acetylation by KAT5 are an essential early step in the DNA damage response (Morillo-huesca *et al.* 2010; Papamichos-Chronakis *et al.* 2011; Xu *et al.* 2012; Gursoy-Yuzugullu *et al.* 2015). H2A.Z must be acetylated and then removed so that KAT5 can acetylate H4 (Bird *et al.* 2002; Downs *et al.* 2004; Doyon *et al.* 2004; Murr *et al.* 2005; Clarke *et al.* 2017). Acetylation of the damage specific phosophorylated histone variant γ-H2A(X) promotes its turnover (Ikura *et al.* 2007; Jha *et al.* 2008; Sharma *et al.* 2010; Soria *et al.* 2012). There is also evidence that NuA4 acetylates the ssDNA binding protein RPA, to regulate resection (Cheng et al. 2018; Kobayashi et al. 2010; Xu et al. 2010). This activity may be important to activate the homologous recombination pathway as opposed to other types of repair (Renaud *et al.* 2015; Jacquet *et al.* 2016).

In fission yeast, Mst1 has multiple activities in chromosome structure, heterochromatin assembly, centromere function, and transcription (Minoda *et al.* 2005; Gómez *et al.* 2008; Kim *et al.* 2009; Nugent *et al.* 2010; Xhemalce and Kouzarides 2010). Previously, we showed that the temperature sensitive mutation *mst1*^{ts} (*mst1*Δ *nmt:mst1-L344S*) results in sensitivity to DNA damaging agents even at permissive temperatures (Gómez et al. 2008; Gómez, Espinosa, and Forsburg 2005). Although we showed that *mst1*$^{+}$ affects transcription of a variety of genes, changes in expression do not appear sufficient to account for its DNA damage sensitivity (Nugent *et al.* 2010). Here, we present evidence that *mst1*$^{+}$ affects DSB repair in fission yeast. We show that Mst1 is recruited to DSB. *mst1-L344S* cells show defects in recruiting downstream factors including Rad52 and RPA. Interestingly, this phenotype is partially rescued by deletion of the end-binding protein Pku70, normally required for NHEJ repair. Our data suggest that Mst1 contributes to efficient resection. Finally, a non-acetylatable H2A.Z mutant (*pht1-4KR*) phenocopies *mst1-L344S*, indicating that H2A.Z may be an important substrate for this effect.

Materials and methods

Strains and Media

Fission yeast cells were grown in YES (yeast extract with supplements) or PMG (pombe minimal glutamate) with appropriate supplements (Sabatinos and Forsburg 2010). Yeast strains used in this research are listed in Supplementary table S2 in the supplemental material.

Serial Dilution plating

Yeast cell cultures were grown at 25ºC in YES for two days. Cultures were diluted in YES to equal concentrations. Five-fold serial dilutions of the cultures were then spotted onto YES plates containing different concentrations of drugs. Plates were incubated at 25ºC or 32ºC for the time indicated in each figure legend.

Determination of DSB-induced recombination rates

DSB-induced recombination outcomes were determined using the strain *ade6-M26 int::pUC8/ura4+/MATa/ade6-L469* described in (Schuchert and Kohli 1988; Fortunato *et al.* 1996). The *S. cerevisiae* homothallic endonuclease (HO) was expressed on a plasmid from the *nmt1* promoter. Cells were first grown up in PMG (pombe minimal glutamate) liquid media lacking uracil and thiamine (PMG -ura -thia) for two days. Cell cultures were then plated onto PMG -ura -leu +thia agar media for five days at 25ºC. After the five-day incubation, colonies were then streaked onto PMG -leu -thia agar media and incubated at 25ºC for seven days (HO expression induced). Three colonies from each induced-break plate were then selected and serially diluted 1:100 in sterile MilliQ H2O. 100µl of the diluted cultures was plated onto PMG low ade -leu -thia agar media. Agar plates were incubated at 25ºC. After the 14-day incubation, red, white and red/white half sectored colonies were counted and marked. Plates were then replica plated onto PMG -leu -ade -thia and PMG

100 -ade, -ura -thia and allowed to grow for another six days at 25ºC before counting colonies with each phenotype.
101 At least three biological replicates were performed. About 8% are likely "complex" rearrangement, for
102 example colonies that were red/white half sectored on PMG low ade -leu -thia agar media. These colonies arise
103 from recombination intermediates that were not repaired before replication (Fortunato *et al.* 1996).

104 **Live-cell imaging and Quantitative Measurements**

105 Live cells imaging was performed as described in (Green *et al.* 2015). Yeast cell cultures were grown
106 at 25ºC in YES overnight. Cells were transferred into PMG + HULAA (Histidine, Uracil, Leucine, Adenine,
107 Arginine) liquid cultures at 25ºC for 16 hours before treating with the indicated drugs for four hours. Cells
108 were collected at OD_{595} 0.3 -0.6, concentrated by centrifuging 1ml at 1500g for 1min and resuspended in 40µl.
109 Concentrated cells were placed on a thin-film pad of 2% agarose in PMG+HULAA on a glass slide. A coverslip
110 was added. Live cells were imaged on DeltaVision Core microscope with softWoRx v4.1 (GE, Issaquah, WA),
111 using a 60X lens, and then deconvolved and projected in softWoRx software. Images were acquired in 13
112 0.2µm z-sections, then deconvolved and Maximum Intensity Projected (softWoRx, default settings). Two
113 separate fields were imaged in each experiment, and 2 to 4 biological replicates were assessed for consistency.
114 Images for publication were contrast adjusted using an equivalent histogram stretch on all samples. Color
115 balance was adjusted, and scale bars were added in Fiji (Schindelin *et al.* 2012). Significance was calculated
116 using the Mann-Whitney U test.

117 **LacO LacI-mCherry DSB array colocalization with CFP-tagged Rad52**

118 Co-localization was performed as described in (Yu *et al.* 2013). Cells were cultured at 25ºC in PMG +
119 HULAA (Histidine, Uracil, Leucine, Adenine, Arginine) +Thiamine liquid media to OD_{595} of 0.4-0.6. Cells
120 were then washed twice with PMG +HULAA medium and incubated at 25ºC for 19 hours to induce HO-driven
121 DSB break. Following induction, cells were collected at OD_{595} of 0.3 to 0.6, and were processed and imaged
122 as described above.

123 **Chromatin Immunoprecipitation (ChIP) assay**

124 Chromatin immunoprecipitation (ChIP) was performed as in (Du *et al.* 2006). Cells were grown in
125 PMG+HULAA+Thiamine overnight to OD_{595}~0.6. Cells were washed 3 times with EMM+HULAA and
126 released in PMG+HULAA-Thiamine at 32ºC with shaking. Samples were taken after washing into
127 PMG+HULAA-Thiamine (T=0), 22hrs(T=22), 24hrs (T=24) and 26hrs (T=26). All samples were fixed with
128 1% formaldehyde for 20min followed by 5 minutes quenching with Glycine. Cells were lysed in standard ChIP
129 buffer and immunoprecipitations were set up using antibodies against GFP (Abcam290), V5(Abcam15828).
130 DNA was column purified using a Qiagen PCR purification kit and qPCR was performed. Fold enrichment
131 was calculated as 100*2^(Adjusted 100% INPUT – Ct(IP)).

132 **Western Blots**

133 For the time course experiment, cells were grown at 32ºC in YES to OD_{595}~0.6 then treated with 40µM
134 camptothecin (CPT) for 4hrs. Cells were washed three times with YES, then released in YES without drug.
135 Time points were taken at T=0 (before addition of drug), T=4 (after 4hrs of drug treatment), and T=6, 8 (two
136 and four hours after removal of drug). Cells were lysed in 20% TCA. Antibodies against phosphorylated H2A
137 (Abcam 17353) and control PCNA (Santa Cruz-56 PC10) were used. For the Chk1-HA phosphorylation
138 experiment, cells were grown at 32ºC in YES to OD_{595}~0.6 then treated for 4hrs with 40µM camptothecin,
139 15mM HU or 0.01%MMS then cells were processed as described above. An anti-HA antibody (12CA5
140 Abcam16918) was used.

141 **Reagent, software, and data availability**

142 All strains and other reagents are available to other investigators upon request. All data are provided
143 within the figures and manuscript or in Supplemental Data uploaded to the GSA Figshare portal. Fig S1: *mst1-*
144 *L344S* sensitivity to phleomycin. S2: Examples of repair protein focus formation in wild type and mutants. S3:
145 *pku70*Δ does not affect cell length. S4: Genetic interactions between *mst1-L344S* and checkpoint mutants.
146 Table S1: Median and quantiles of data in Fig 2A and B. S2: Strain list.

147

148 **Results**

149 **Mst1 is important for double-strand break repair in *S. pombe***

150 Mst1 homologs in mammalian cells (TIP60) and *S. cerevisiae* (*ESA1*) are known to be important for
151 DSB repair (rev. in (Ghobashi and Kamel 2018; Van and Santos 2018; Clouaire and Legube 2019; Aleksandrov
152 *et al.* 2020)). We have previously shown that a *S. pombe mst1*$^+$ temperature sensitive allele (*mst1-L344S*)
153 renders cells sensitive to various DNA damaging drugs (Gómez *et al.* 2008). Here we expand these studies to
154 further dissect the role of *mst1*$^+$ in DSB repair.

155 Our original *mst1-L344S* construct is expressed from the *nmt1* promoter inserted at the *leu1*$^+$ locus in
156 a deletion background (*mst1*Δ *nmt:mst1-L344S* Gómez et al. 2008) but subsequently, the same allele was
157 engineered at the native locus under control of the endogenous *mst1*$^+$ promoter (*mst1-L344S* Garabedian et al.
158 2012). We tested the sensitivity of both versions to bleomycin, which creates single and double strand DNA
159 breaks (Stubbe and Kozarich 1987; Burger 1998). Both these strains were modestly sensitive to the drugs at
160 25ºC (Figure 1A; Gómez et al. 2008), consistent with a requirement for Mst1 in DSB repair. Because the *mst1-*
161 *L344S* allele does not generate autofluorescence to the same extent as our original allele, we employed it here
162 for visual assays.

163 We investigated the role of *mst1*$^+$ in repair of a single DSB break. We first utilized a strain that uses
164 the homothallic switching endonuclease (HO) to induce a single DSB between two non-tandem repeats as
165 originally described by (Schuchert and Kohli 1988) and modified by (Osman *et al.* 2000) (Figure 1B). In this

166 strain, a functional *ura4*$^{+}$ gene is flanked by two full length non-functional *ade6* alleles, each containing a
167 different point mutation. The HO endonuclease makes a DSB at *MATa* site adjacent to *ura4*$^{+}$. The repair
168 outcomes can be determined by selecting Ade^{+} cells and screening for Ura^{+} (Fortunato *et al.* 1996; Osman *et*
169 *al.* 1996, 2000; Ahn *et al.* 2005). Uracil auxotrophic colonies ("deletion type", whether Ade^{+} or Ade^{-}) result
170 from deletion and rearrangement, in which cells repaired the lesion by Single Strand Annealing (SSA), Non-
171 Homologous End-Joining (NHEJ), or more complex rearrangements. In contrast, Ade^{+} colonies that retain
172 Ura+ ("conversion type") are presumed to derive from gene conversion via homologous recombination.

173 Following induction of the DSB, we observed that the survival of *mst1-L344S* was much lower than
174 the survival in wild-type cells (Figure 1C), consistent with a repair defect. In wild-type cells, about 55.64% of
175 colonies are deletion type (Ade+/Ade- Ura-) while 36.70% of colonies were conversion type (Ade+ Ura+)
176 (Figure 1D). In the surviving *mst1-L344S* cells, we observed a significantly higher percentage of colonies
177 showing deletion-type repair (75.3%) than in wild type (Figure 1D). These data suggest that wild type *mst1*$^{+}$
178 biases repair towards conversion-type, error-free recombination.

179 To examine whether Mst1 physically localizes to DSB breaks as has been reported for *Hs*TIP60 and
180 *Sc*Esa1 (Downs and Jackson 2004; Sun *et al.* 2009), we employed a strain previously engineered to test
181 recruitment of proteins by ChIP to one single double strand break (Figure 1E) (Du *et al.* 2006). This assay can
182 monitor both temporal and spatial recruitment of proteins to a single DSB. We detected Mst1 localized near
183 the DSB after induction, although the level of enrichment was lower than that of Rad52 (Figure 1E, note two
184 different Y-axes for Mst1 and Rad52). As expected, Mst1 localization to sequences near DSB was reduced in
185 cells missing H3K9 methyltransferase Clr4 (Figure 1E), which is consistent with previous finding that
186 *Hs*TIP60 binds to the DSB via H3K9^{me} (Sun et al. 2005; Sun et al. 2009, Ayrapetov et al. 2014). Additionally,
187 Rad52 localization to the DSB was reduced in *clr4*Δ (Figure 1E and F), consistent with findings in human cells
188 that H3K9^{me}-deficient cells had reduced homologous recombination-mediated repair (Ayrapetov *et al.* 2014,
189 Sun et al. 2009).

190 **Mst1 contributes to recruitment of repair factors to DSBs**

191 Consistent with a role for Mst1 in DSB repair, we found that the mutant *mst1* at permissive temperature
192 is modestly sensitive to agents that induce DSBs, including the radiomimetic drugs Bleomycin and its analogue
193 Phleomycin (Belenguer et al. 1995) (Figure 1A, supplementary figure 1), suggesting this mutant has attenuated
194 function even under permissive conditions. We next examined the recruitment of homologous recombination
195 proteins in *mst1-L344S* cells using a visual screen following treatment with phleomycin. First, we looked at
196 the localization of RPA and Rad52 proteins (Figure 2A, supplementary table 1). Untreated wild type and *mst1*
197 cells had a similar percentage of cells with foci. However, following phleomycin treatment, we observed
198 significantly more cells with foci in wild type than in *mst1-L344S* cells. We also imaged cells with GFP-tagged

199 Rad54, a recombination protein that acts downstream of Rad52 (Figure 2B; Onaka et al. 2016). Similar to RPA
200 and Rad52, the fraction of *mst1-L344S* cells with Rad54 foci was lower than in the wild type strain (Figure 2B,
201 supplementary table 1). These observations suggest that Mst1 is required for the normal recruitment of
202 downstream HR factors.

203 Next, we examined the recruitment of Rad52 at a single, induced DSB site. We utilized a strain that
204 contains an HO-inducible DSB adjacent to a lacO array that recruits mCherry-lacI, and CFP-tagged Rad52
205 (Yu *et al.* 2013). We imaged both wild-type and *mst1-L344S* cells over a four-hour period. In wild-type cells,
206 we observed that 75% of total Rad52 foci co-localize with mCherry signal until 100 minutes (Figure 2C top).
207 After 100 minutes, the percentage of colocalization dropped in wild type, because the mCherry-LacI signal
208 disappears (Figure 2C bottom and Figure 2D). This loss of mCherry-lacI likely reflects resection at DSBs that
209 eliminates the LacO target, as shown previously (Yu *et al.* 2013; Leland *et al.* 2018). Consistent with these
210 prior reports, we observed that the mCherry-DSB foci dropped to 25% by the end of four-hour time-course
211 (Figure 2D, Yu et al. 2013). In contrast, in *mst1-L344S* cells, fewer than 40% of total Rad52 foci colocalize
212 with mCherry-DSB foci across the four-hour time-course, suggesting Mst1 is involved in Rad52 recruitment
213 (Figure 2C top). Strikingly, however, over 90% of mCherry-DSB signal remained even at the end of the time-
214 course (Figure 2C bottom and Figure 2D). This suggests that in the absence of functional Mst1, resection is
215 inhibited, so the LacI-mcherry bound to the lacO array persists.

216 **Processing of DSBs and a role for Ku**

217 The heterodimeric Ku complex is very abundant and binds rapidly and immediately to DSBs (Fell and
218 Schild-Poulter 2015; Shibata *et al.* 2018). Ku inhibits initial resection driven by MRN, while MRN removes
219 Ku to promote proper resection and facilitate homologous recombination (HR) (Tomita *et al.* 2003; Langerak
220 *et al.* 2011; Shao *et al.* 2012; Myler *et al.* 2017; Shibata *et al.* 2018). Unexpectedly, we found that *pku70*Δ
221 partially rescues the bleomycin sensitivity of *mst1*Δ *mst1-L344S* (Figure 3A).

222 We wondered whether Pku70 also affects the recruitment of repair proteins in *mst1-L344S*, so we
223 imaged fluorescently tagged RPA under phleomycin treatment. We observed first that the percentage of
224 untreated cells with RPA foci in *pku70*Δ and *pku70*Δ *mst1-L344S* is higher than in wild type or *mst1-L344S*
225 (Figure 2A, supplementary figure 2, supplementary table 1), suggesting a burden of endogenous damage.
226 However, cell growth and cell length at septation were not significantly affected (Figure 3A, supplementary
227 figure 3).

228 Upon treatment, the number of positive cells is only slight increased, and does not reach the level
229 observed in wild-type cells (Figure 2A, supplementary figure 2A, supplementary table 1). Results were slightly

230 different for Rad52: the *pku70*Δ single mutant cells showed a comparable level to wild type in untreated
231 conditions, with little change following treatment. The untreated double mutant *pku70*Δ *mst1-L344S* were
232 higher than either single mutant and showed a modest increase upon treatment, but not to the levels of wild
233 type (Figure 2A, supplementary figure 2A, supplementary table 1). Finally, the fraction of *pku70*Δ with Rad54
234 foci is similar to wild type in untreated cells, increased by the same relative proportion following treatment.
235 Again, the untreated *mst1-L344S pku70*Δ has a higher baseline in untreated cells than either single mutant, and
236 induces to approximately wild type levels (Figure 2B, supplementary figure 2C, supplementary table 1).

237 We used the mCherry-LacI marked HO-induced DSB system to examine the apparent resection of DSB
238 in *pku70*Δ mutants by monitoring the disappearance of mCherry signal (Figure 2D). We find that *pku70*Δ
239 single mutant cells do show a slight reduction in mCherry-DSB foci over time, but this effect is far more
240 modest than that in wild-type. At the end of the time-course, just under 70% of the *pku70*Δ cells still contain
241 mCherry-DSB foci. We observed a similar phenotype in *pku70*Δ *mst1-L344S* cells. (Figure 2D).

242 Long range resection is initiated by MRN and extended by the exonuclease Exo1, as well as other
243 proteins (Zhu *et al.* 2008; Langerak *et al.* 2011; Yan *et al.* 2019). We observed that mCherry-LacI marked
244 DSBs do not disappear over the time-course in *exo1*Δ, in contrast to wild-type (Figure 2D), and consistent with
245 a failure in resection. We observed that *exo1*Δ*, mst1-L344S,* and the double mutant *exo1*Δ *mst1-L344S* all show
246 a similar persistence of the mCherry signal. Additionally, *exo1*Δ *mst1-L344S* has similar sensitivity to
247 bleomycin as the *mst1-L344S* single mutant and this sensitivity is rescued by *pku70*Δ (Figure 3A). These data
248 suggest that $mst1^+$ and $exo1^+$ are in the same pathway.

249 **Is H2A.Z a target of Mst1 to regulate DSB repair**?

250 In other organisms that the presence and turnover of the histone variant H2A.Z (*S. pombe* Pht1), a
251 KAT5 substrate, is important for the proper repair of DSBs by regulating resection (Xu *et al.* 2012; Gursoy-
252 Yuzugullu *et al.* 2015; Jiang *et al.* 2015). In human cells, H2A.Z depletion leads to higher ssDNA accumulation
253 and lower DSB recovery from HR (Xu *et al.* 2012; Jiang *et al.* 2015). Failure to remove H2A.Z at DSBs in
254 human cells leads to higher RPA binding and higher recovery from HR (Gursoy-Yuzugullu *et al.* 2015). In
255 fission yeast, H2A.Z is a known substrate of Mst1, and a mutant *pht1-4KR* that disrupts the Mst1 acetylation
256 sites causes genome instability and anaphase defects (Kim *et al.* 2009). To investigate the role of H2A.Z
257 acetylation in repair, we compared the phenotype of *pht1-4KR* and *pht1*Δ to *mst1-L344S.* We observed
258 significant reduction in RPA and Rad52 foci in *pht1-4KR* at 25ºC similar to that observed with *mst1-L344S*
259 cells (Figure 2A, supplementary figure 2B, supplementary table 1). However, in contrast to *mst1-L344S,* the
260 sensitivity to bleomycin we observe in *pht1-4KR* is not rescued by *pku70*Δ (Figure 3B).

261 We also compared the phenotypes of *pht1*Δ and *pht1-4KR* cells. *pht1*Δ showed fewer cells with RPA
262 foci compared to wild type under phleomycin treatment (Figure 2A, supplementary figure 2B, supplementary
263 table 1). Rad52 foci were also reduced in *pht1*Δ compared to wild type under phleomycin treatment (Figure
264 2A). However, the effect of *pht1-4KR* cells was more dramatic than *pht1*Δ, and much closer to the observations
265 in *mst1-L344S* (Figure 2A, supplementary table 1). Finally, we used the mCherry-DSB reporter system to
266 examine resection *in vivo*. As with *mst1-L344S* and *exo1*Δ, *pht1-4KR* cells showed a persistent mCherry-DSB
267 signal, consistent with a failure to resect (Figure 2D).

268 **The damage checkpoint is normal in *mst1-L344S***

269 Previously, we showed that the temperature-sensitive allele *mst1*Δ *leu1*$^{+}$*::nmt-mst1-L344S* is sensitive
270 to S-phase specific genotoxins including methyl methanesulfonate (MMS), which causes alkylation damage
271 that inhibits replication, and camptothecin (CPT), a topoisomerase-I inhibitor that causes lesions during S-
272 phase (Wan *et al.* 1999; Fung *et al.* 2002; Morishita *et al.* 2003; Frampton *et al.* 2006). In contrast to our
273 observations with phleomycin, which induces general DSBs, we observed that the percentage of cells with
274 RPA and Rad52 foci was higher in *mst1-L344S* cells treated with these S-phase specific genotoxins than that
275 in wild-type (Figure 4A). This is consistent with these S-phase specific lesions inducing different repair
276 pathways, including post-replication repair via translesion synthesis and template switching to repair MMS-
277 induced damage, as well as nucleolytic cleavage of protein -DNA adducts to repair CPT-induced damages (rev.
278 in (Alagoz et al. 2012; Arbel, Liefshitz, and Kupiec 2020)).

279 We examined genetic interactions between *mst1-L344S* and mutants that affect checkpoint under
280 treatment with a variety of S-phase specific genome stressors (Supplementary figure 4). A modest growth
281 defect in untreated cells was observed for the double mutant *mst1-L344S rad3*Δ but not for others. In cells
282 treated with UV or MMS at 25ºC, we observed a striking negative interaction between *mst1-L344S* and damage
283 checkpoint mutants *chk1*Δ or *crb2*Δ at 25ºC, suggesting a requirement for an active damage checkpoint
284 response under these treatments. This data is consistent with previous findings in *S. cerevisiae* that the cell
285 cycle delay in NuA4 mutant depends on Rad9 (*Sp*Crb2 ortholog) after DSB induction (Javaheri *et al.* 2006).
286 We treated cells with MMS, CPT or hydroxyurea (HU) and performed western blots against HA tagged Chk1.
287 In wild-type, Chk1 is phosphorylated in cells treated with four-hour CPT or MMS, but not in untreated cells
288 or cells treated with HU (Figure 4B; Walworth and Bernards 1996). We observed a largely similar
289 phosphorylation pattern in *mst1-L344S* mutant (Figure 4B), although there may be a modest reduction in the
290 amount of pChk1. H2A phosphorylation, one of the first sensors of DNA damage and double strand breaks,
291 was also present in *mst1-L344S* cells after 4-hour CPT treatment as in wild-type cells and diminished after
292 removing drugs from cell culture (Figure 4C). Mst1 is not required for checkpoint activation in response to S-
293 phase specific lesions but depends on that response for viability.

294

295 **Discussion**

296 The MYST protein Mst1 (hTIP60; ScEsa1; KAT5) is the catalytic subunit of the NuA4 histone
297 acetyltransferase complex, and makes pleiotropic contributions to genome stability (rev. in (Lafon *et al.* 2007;
298 Pillus 2008)). Multiple studies indicate that hTIP60 and ScEsa1 contribute to DSB repair through acetylation
299 (rev. in (Ghobashi and Kamel 2018)), and show that the acetyltransferase binds near DSB regions (Downs *et*
300 *al.* 2004; Sun *et al.* 2009; Xu *et al.* 2010; Li and Wang 2017; Cheng *et al.* 2018). The budding yeast ScEsa1
301 acetylates ssDNA binding protein RPA at DSBs (Cheng *et al.* 2018) and in mammalian cells, TIP60 promotes
302 HR localization of recombination protein Rad51 (Murr *et al.* 2005).

303 Previously we showed that Mst1 is *S. pombe* is essential for viability and we demonstrated the
304 temperature sensitive allele *mst1-L344S* is sensitive to a number of genotoxins (Gómez et al. 2008; Gómez,
305 Espinosa, and Forsburg 2005). Here, we confirmed that Mst1 in *S. pombe* is important for DSB repair because
306 both temperature sensitive alleles are sensitive to a DSB-inducing environment including treatment with
307 phleomycin or bleomycin, or constitutive HO-nuclease expression (Figure 1A, 1C, 3 and supplementary figure
308 1). We find that Mst1 directly localizes to DSBs, and this localization depends on H3K9^{me} (Figure 1E and
309 Figure 5). We observe that even under permissive growth conditions, *mst1-L344S* shifts the balance of repair
310 away from HR towards SSA or NHEJ (Figure 1D). We also observed that a lower percentage of *mst1-L344S*
311 cells compared to wild type show visible foci of HR associated proteins RPA, Rad52 or Rad54, following
312 treatment with DSB inducing agents (Figure 2A, B). Together, these observations suggest that Mst1 facilitates
313 homologous recombination to repair DSBs, and in its absence, HR is impaired (Figure 5).

314 There are conflicting data as to whether KAT5/NuA4 influences non-homologous end joining (NHEJ),
315 which is typically the alternative pathway for repair if HR is inhibited (Chang *et al.* 2017). In budding yeast,
316 ScEsa1 has been reported to be essential for NHEJ at DSBs (Bird *et al.* 2002). However, studies in mammalian
317 cells suggest TIP60 instead inhibits NHEJ by acetylating H2A and H4; this reduces loading of 53BP1 protein
318 that promotes NHEJ (Tang *et al.* 2013; Renaud *et al.* 2015; Jacquet *et al.* 2016). Consistent with this, in
319 budding yeast deletion of the 53BP1 orthologue Sc*rad9* increases resection efficiency (Bonetti *et al.* 2015) and
320 similarly, fission yeast *crb2*Δ mutants have increased resection (Leland *et al.* 2018). However, in fission yeast,
321 the G2-dominant cell cycle means that NHEJ is generally not the preferred pathway for DSB repair in growing
322 cells (rev. in (Langerak and Russell 2011)). Because of this, we did not specifically examine efficiency of
323 NHEJ. Our data suggest that Mst1 affects homologous recombination, specifically by reducing long-range
324 resection (Figure 2 and Figure 5).

325 To monitor resection, we used a visual assay in which a lacO array marked by lacI-mCherry is adjacent
326 to an induced double strand break. Previous studies have shown that loss of the lacO array adjacent to a break
327 correlates with resection (Yu *et al.* 2013; Leland *et al.* 2018). Consistent with this, we find that the mCherry
328 signal declines over time in a wild type in the presence of the induced break, but not in an *exo1*Δ mutant that
329 lacks the long-range exonuclease. We also observe that *mst1-L344S* resembles *exo1*Δ in this assay. The data
330 from this, as well as the mutant sensitivity to DSB-inducing drugs, suggest that *mst1* and *exo1* are in a common
331 epistasis group (Figure 5).
332 The end-binding protein complex Ku inhibits resection and thus, homologous recombination (rev. in
333 (Shibata, Jeggo, and Löbrich 2018)). Its activity is coordinated with the Mre11-Rad50-Nbs1 (MRN) complex
334 associated with early steps in resection (rev. in (Shibata, Jeggo, and Löbrich 2018; Syed and Tainer 2018)).
335 While Ku inhibits resection driven by MRN, MRN removes Ku to facilitate homologous recombination (HR)
336 over NHEJ (Langerak and Russell 2011; Shao *et al.* 2012; Myler *et al.* 2017; Shibata *et al.* 2018). Previous
337 work has shown that *pku70*Δ rescues some resection in the absence of the MRN complex (Tomita *et al.* 2003;
338 Langerak *et al.* 2011; Teixeira-Silva *et al.* 2017). Consistent with these observations, we found *pku70*Δ also
339 partially rescues *mst1* and *mst1 exo1*Δ sensitivity to DSB-inducing agents, and partly restores recruitment of
340 HR proteins and resection. This agrees with a model that Pku70 inhibits an alternative resection pathway that
341 is independent of MRN, Mst1, or Exo1.
342 However, we observe an intermediate effect of Pku70 on resection in our visual assay: unexpectedly
343 *pku70*Δ showed stabilization of the mCherry-LacI signal in both wild type and *mst1-L344S* backgrounds,
344 whereas we expected at least the single mutant to show wild type levels of resection. Since Pku70 represses
345 microhomology-mediated end joining (MMEJ), one possibility is that an increase of MMEJ antagonizes
346 resection directly (Decottignies 2007; Wang and Xu 2017). This may also distinguish a role for Ku in the
347 initiation of resection (which is Exo1-independent) from long range resection, which is likely required to see
348 loss of the mCherry-LacI signal and could be antagonized by MMEJ in our assay. Ku also plays a role in
349 telomere maintenance (Baumann and Cech 2000; Manolis *et al.* 2001), in replication fork restart (Teixeira-
350 Silva *et al.* 2017), and in rDNA stability (Miyoshi *et al.* 2009; Sánchez and Russell 2015). It represses
351 chromosome rearrangements (Prudden *et al.* 2003). We observed increased RPA signal in the *pku70*Δ mutant
352 without any treatment, suggesting the loss of Pku70 causes an increased burden of ssDNA. It is possible that
353 efficiency of resection at a single engineered break is reduced due to recruitment of resection activities to
354 numerous other sites of genotoxic stress that are the result of Ku depletion, but this observation will require
355 further analysis.
356 Multiple studies show the presence and the turnover of the histone variant H2A.Z (SpPht1) is required
357 for DSB repair (Kalocsay *et al.* 2009; Xu *et al.* 2012; Gursoy-Yuzugullu *et al.* 2015; Jiang *et al.* 2015). In

358 mammalian cells, the absence of H2A.Z leads to more ssDNA accumulation and reduced Pku70 localization
359 (Xu *et al.* 2012; Gursoy-Yuzugullu *et al.* 2015). Exchange of H2A.Z is required for H4 acetylation by TIP60,
360 which creates open chromatin (Gursoy-Yuzugullu, Ayrapetov, and Price 2015; Xu et al. 2010, 2012). Several
361 acetyltransferases have been implicated in H2A.Z acetylation including KAT5 (Mst1) and KAT2A (Gcn5)
362 (Kusch *et al.* 2004; Babiarz *et al.* 2006; Keogh *et al.* 2006; Millar *et al.* 2006; Zlatanova and Thakar 2008;
363 Kim *et al.* 2009; Semer *et al.* 2019). In mammalian cells, the deposition of H2A.Z precedes its acetylation (Xu
364 *et al.* 2012), while in Drosophila, the acetylation of H2A.Z homolog H2Av stimulates its removal after DNA
365 damage (Kusch *et al.* 2004). Blocking TIP60 prevents both H2A.Z exchange and H4 acetylation (Morillo-
366 huesca *et al.* 2010; Papamichos-Chronakis *et al.* 2011; Xu *et al.* 2012; Shastri *et al.* 2018).

367 To investigate whether H2A.Z acetylation by Mst1 influences repair, we used a non-acetylable mutant
368 of H2A.Z, *pht1-4KR*. This mutation has previously been shown to disrupt Mst1 acetylation sites and leads to
369 chromosome segregation errors (Kim *et al.* 2009). We saw a similar percentage of *pht1-4KR* cells with RPA
370 and Rad52 foci as seen in *mst1-L344S* cells in treated cells, both significantly lower than that in wild type.
371 Additionally, mCherry-DSB foci in *pht1-4KR* did not disappear across the time-course, and the percentage of
372 mCherry-DSB persistence was similar to that in *mst1-L344S* (Figure 2D). This suggests that *pht1-4KR* and
373 *mst1-344S* affect in a common pathway required for resection. We speculate that *pht1-4KR* once inserted
374 cannot be efficiently removed, and interferes with H4 acetylation and chromatin decompaction. This would
375 essentially lock the chromatin in a form refractory to long range resection. This could explain why sensitivity
376 of *pht1-4KR* to DSBs is more severe than that of *pht1*Δ, suggesting that an immobile H2A.Z is more damaging
377 than no H2A.Z at all. However, in contrast to *mst1*, *pht1-4KR* sensitivity to bleomycin is not rescued by *pku70*Δ
378 (Figure 3B). This might suggest that H2A.Z binds to DSBs after Pku70 is removed, but that would be
379 inconsistent with work in mammalian cells suggesting that Ku-recruitment is H2A.Z dependent (Xu *et al.*
380 2012). Further work will be required to resolve these observations.

381 Finally, we show that the temperature sensitive allele *mst1*Δ *leu1*$^{+}$*::nmt:mst1-L344S* is sensitive to S
382 phase specific genotoxins including methyl methanesulfonate (MMS) and camptothecin (CPT) even at
383 permissive temperature (Gómez et al. 2008). This is consistent with a recent study showing that Mst1 in *S.*
384 *pombe* is important for CPT-induced damge repair (Noguchi *et al.* 2019). Studies in *S. cerevisiae* showed
385 Esa1's importance to MMS-induced damage repair through translesion synthesis and sister chromatid
386 recombination (Bird *et al.* 2002; House *et al.* 2014; Renaud-Young *et al.* 2015). Compromised DNA damage
387 repair could be the result of defective damage checkpoint activation. In mammalian cells, TIP60 is known to
388 acetylate ATM and p53 (Sun *et al.* 2005; Sykes *et al.* 2006; Tang *et al.* 2006). However, we find that the
389 temperature sensitive allele does not affect activation of DNA damage checkpoint Chk1 or phosphorylation of
390 H2A(X) (Figure 4B and C).

391 Taken together, our data suggest that SpMst1contributes to repair of a variety of DNA lesions. As in
392 other organisms, our data show that Mst1 acetyltransferase has a particular role in double strand break repair,
393 where it facilitates homologous recombination by promoting long range resection and antagonizing NHEJ-
394 promoting factors such as Ku (Figure 5). Our data suggest that this depends on acetylation of H2A.Z. The
395 conservation of function of this acetyltransferase across eukaryotes indicates the fundamental nature of
396 chromatin modification in DNA repair transactions.
397

398 **Acknowledgement**

399 We would like to thank Li-Lin Du, Michael Keogh, Takuro Nakagawa, Eishi Noguchi, Mathew
400 O'Connell, and Simon Whitehall for strains. We thank Ji-Ping Yuan and Amanda Jensen for assistance and
401 technical support. We are grateful to current members of the Forsburg lab for many helpful comments and
402 discussions throughout the course of the study, and an anonymous reviewer for helpful suggestion. This work
403 was supported by NIH R35 GM118109 (SLF).
404

405 **References**

406 Ahn J. S., F. Osman, and M. C. Whitby, 2005 Replication fork blockage by RTS1 at an ectopic site promotes
407 recombination in fission yeast. EMBO J. 24: 2011–2023. https://doi.org/10.1038/sj.emboj.7600670
408 Alagoz M., D. C. Gilbert, S. El-Khamisy, and A. J. Chalmers, 2012 DNA Repair and Resistance to
409 Topoisomerase I Inhibitors: Mechanisms, Biomarkers and Therapeutic Targets. Curr. Med. Chem. 19:
410 3874–3885. https://doi.org/10.2174/092986712802002590
411 Aleksandrov R., R. Hristova, S. Stoynov, and A. Gospodinov, 2020 The Chromatin Response to Double-
412 Strand DNA Breaks and Their Repair. Cells 9. https://doi.org/10.3390/cells9081853
413 Allard S., R. T. Utley, J. Savard, A. Clarke, P. Grant, *et al.*, 1999 The NuA4 transcription activation/histone
414 H4 acetyltransferase complex contains the essential Esa1 protein as the catalytic subunit and the
415 essential ATM-related cofactor Tra1p. Biochem. Cell Biol. 77: 5108–5119. https://doi.org/10.1139/o99-
416 903
417 Arbel M., B. Liefshitz, and M. Kupiec, 2020 How yeast cells deal with stalled replication forks. Curr. Genet.
418 66: 911–915. https://doi.org/10.1007/s00294-020-01082-y
419 Avvakumov N. ., and J. Côté, 2007 The MYST family of histone acetyltransferases and their intimate links
420 to cancer. Oncogene 26: 5395–5407. https://doi.org/10.1038/sj.onc.1210608
421 Ayrapetov M. K., O. Gursoy-Yuzugullu, C. Xu, Y. Xu, and B. D. Price, 2014 DNA double-strand breaks
422 promote methylation of histone H3 on lysine 9 and transient formation of repressive chromatin. Proc.
423 Natl. Acad. Sci. 111: 9169–9174. https://doi.org/10.1073/pnas.1403565111
424 Babiarz J. E., J. E. Halley, and J. Rine, 2006 Telomeric heterochromatin boundaries require NuA4-dependent
425 acetylation of histone variant H2A.Z in Saccharomyces cerevisiae. Genes Dev.
426 https://doi.org/10.1101/gad.1386306
427 Bakkenist C. J., and M. B. Kastan, 2015 Chromatin perturbations during the DNA damage response in
428 higher eukaryotes. DNA Repair (Amst). 36: 8–12. https://doi.org/10.1016/j.dnarep.2015.09.002
429 Baumann P., and T. R. Cech, 2000 Protection of telomeres by the Ku protein in fission yeast. Mol. Biol.
430 Cell. https://doi.org/10.1091/mbc.11.10.3265
431 Belenguer P., M.-L. Oustrin, G. Tiraby, and B. Ducommun, 1995 Effects of phleomycin-induced DNA
432 damage on the fission yeast Schizosaccharomyces pombe cell cycle. Yeast 11: 225–231.
433 https://doi.org/10.1002/yea.320110305
434 Bird A. W., D. Y. Yu, M. G. Pray-Grant, Q. Qiu, and M. F. Christman, 2002 Acetylation of histone H4 by
435 Esa1 is required for DNA double-strand break repair. Nature 419: 411–415.
436 https://doi.org/10.1038/nature01080.Published
437 Bonetti D., M. Villa, E. Gobbini, C. Cassani, G. Tedeschi, *et al.*, 2015 Escape of Sgs1 from Rad9 inhibition

438 reduces the requirement for Sae2 and functional MRX in DNA end resection . EMBO Rep. 16: 351–
439 361. https://doi.org/10.15252/embr.201439764
440 Burger R. M., 1998 Cleavage of Nucleic Acids by Bleomycin. 2665: 16–19.
441 https://doi.org/10.1021/cr960438a
442 Chang H. H. Y., N. R. Pannunzio, N. Adachi, and M. R. Lieber, 2017 Non-homologous DNA end joining
443 and alternative pathways to double-strand break repair. Nat. Rev. Mol. Cell Biol. 18: 495–506.
444 https://doi.org/10.1038/nrm.2017.48
445 Cheng X., O. Jobin-robitaille, P. Billon, R. Buisson, V. Côté, *et al.*, 2018 Phospho-dependent recruitment of
446 NuA4 by MRX at DNA breaks regulates RPA dynamics during resection. Proc. Natl. Acad. Sci. U. S.
447 A. 6: P93. https://doi.org/10.1186/1756-8935-6-S1-P93
448 Clarke T. L. ., M. P. Sanchez-Bailon, K. Chiang, J. J. . Reynolds, J. Herrero-Ruiz, *et al.*, 2017 PRMT5-
449 Dependent Methylation of the TIP60 Coactivator RUVBL1 Is a Key Regulator of Homologous
450 Recombination. Mol. Cell 65: 900–916. https://doi.org/10.1016/j.molcel.2017.01.019
451 Clouaire T., and G. Legube, 2019 A Snapshot on the Cis Chromatin Response to DNA Double-Strand
452 Breaks. Trends Genet. 35: 330–345. https://doi.org/10.1016/j.tig.2019.02.003
453 Decottignies A., 2007 Microhomology-mediated end joining in fission yeast is repressed by Pku70 and relies
454 on genes involved in homologous recombination. Genetics 176: 1403–1415.
455 https://doi.org/10.1534/genetics.107.071621
456 Dhar S., O. Gursoy-Yuzugullu, R. Parasuram, and B. D. Price, 2017 The tale of a tail: Histone H4
457 acetylation and the repair of DNA breaks. Philos. Trans. R. Soc. B Biol. Sci. 372.
458 https://doi.org/10.1098/rstb.2016.0284
459 Downs J. A., S. Allard, O. Jobin-Robitaille, A. Javaheri, A. Auger, *et al.*, 2004 Binding of chromatin-
460 modifying activities to phosphorylated histone H2A at DNA damage sites. Mol. Cell 16: 979–990.
461 https://doi.org/10.1016/j.molcel.2004.12.003
462 Downs J. A., and S. P. Jackson, 2004 A means to a DNA end: The many roles of Ku. Nat. Rev. Mol. Cell
463 Biol. 5: 367–378. https://doi.org/10.1038/nrm1367
464 Doyon Y., and J. Côté, 2004 The highly conserved and multifunctional NuA4 HAT complex. 2 14: 147–154.
465 https://doi.org/10.1016/j.gde.2004.02.009
466 Doyon Y., W. Selleck, W. S. Lane, S. Tan, and J. Côté, 2004 Structural and functional conservation of the
467 NuA4 histone acetyltransferase complex from yeast to humans. Mol. Cell. Biol. 24: 1884–96.
468 https://doi.org/10.1128/MCB.24.5.1884
469 Du L. L., T. M. Nakamura, and P. Russell, 2006 Histone modification-dependent and -independent pathways
470 for recruitment of checkpoint protein Crb2 to double-strand breaks. Genes Dev. 20: 1583–1596.

471 https://doi.org/10.1101/gad.1422606
472 Fell V. L., and C. Schild-Poulter, 2015 The Ku heterodimer: Function in DNA repair and beyond. Mutat.
473 Res. - Rev. Mutat. Res. 763: 15–29. https://doi.org/10.1016/j.mrrev.2014.06.002
474 Fortunato E. A., F. Osman, and S. Subramani, 1996 Analysis of spontaneous and double-strand break-
475 induced recombination in rad mutants of S. pombe. Mutat. Res. - DNA Repair 364: 147–160.
476 https://doi.org/10.1016/S0921-8777(96)00022-5
477 Frampton J., A. Irmisch, C. M. Green, A. Neiss, M. Trickey, *et al.*, 2006 Postreplication Repair and PCNA
478 Modification in Schizosaccharomyces pombe. Mol. Biol. Cell 17: 2976–2985.
479 https://doi.org/10.1091/mbc.E05
480 Fung A. D., J. Ou, S. Bueler, and G. W. Brown, 2002 A Conserved Domain of Schizosaccharomyces pombe
481 dfp1+ Is Uniquely Required for Chromosome Stability following Alkylation Damage during S Phase.
482 Mol. Cell. Biol. 22: 4477–4490. https://doi.org/10.1128/mcb.22.13.4477-4490.2002
483 Galarneau L., A. Nourani, A. A. Boudreault, Y. Zhang, L. Héliot, *et al.*, 2000 Multiple links between the
484 NuA4 histone acetyltransferase complex and epigenetic control of transcription. Mol. Cell.
485 https://doi.org/10.1016/S1097-2765(00)80258-0
486 Garabedian M. V., C. Noguchi, M. A. Ziegler, M. M. Das, T. Singh, *et al.*, 2012 The double-bromodomain
487 proteins Bdf1 and Bdf2 modulate chromatin structure to regulate S-phase stress response in
488 schizosaccharomyces pombe. Genetics 190: 487–500. https://doi.org/10.1534/genetics.111.135459
489 Ghobashi A. H., and M. A. Kamel, 2018 Tip60 : updates. Hum. Genet. 59: 161–168.
490 Gómez E. B., J. M. Espinosa, and S. L. Forsburg, 2005 Schizosaccharomyces pombe mst2+ encodes a
491 MYST family histone acetyltransferase that negatively regulates telomere silencing. Mol. Cell. Biol. 25:
492 8887–8903. https://doi.org/10.1128/MCB.25.20.8887-8903.2005
493 Gómez E. B., R. L. Nugent, S. Laria, and S. L. Forsburg, 2008 Schizosaccharomyces pombe histone
494 acetyltransferase Mst1 (KAT5) is an essential protein required for damage response and chromosome
495 segregation. Genetics 179: 757–771. https://doi.org/10.1534/genetics.107.085779
496 Green M. D. ., S. A. . Sabatinos, and S. L. . Forsburg, 2015 Microscopy Techniques to Examine DNA
497 Replication in Fission Yeast. Methods Mol Biol 1300: 13–41. https://doi.org/10.1016/B978-0-12-
498 374984-0.00431-9
499 Gursoy-Yuzugullu O., M. K. . Ayrapetov, and B. D. . Price, 2015 Histone chaperone Anp32e removes
500 H2A.Z from DNA double-strand breaks and promotes nucleosome reorganization and DNA repair.
501 Proc. Natl. Acad. Sci. 112: 7507–7512. https://doi.org/10.1073/pnas.1504868112
502 House N. C. M., J. H. Yang, S. C. Walsh, J. M. Moy, and C. H. Freudenreich, 2014 NuA4 Initiates Dynamic
503 Histone H4 Acetylation to Promote High-Fidelity Sister Chromatid Recombination at Postreplication

504 Gaps. Mol. Cell 55: 818–828. https://doi.org/10.1016/j.molcel.2014.07.007
505 Ikura T., S. Tashiro, A. Kakino, H. Shima, N. Jacob, *et al.*, 2007 DNA Damage-Dependent Acetylation and
506 Ubiquitination of H2AX Enhances Chromatin Dynamics. Mol. Cell. Biol. 27: 7028–7040.
507 https://doi.org/10.1128/MCB.00579-07
508 Jacquet K., A. Fradet-Turcotte, N. Avvakumov, J. P. Lambert, C. Roques, *et al.*, 2016 The TIP60 Complex
509 Regulates Bivalent Chromatin Recognition by 53BP1 through Direct H4K20me Binding and H2AK15
510 Acetylation. Mol. Cell 62: 409–421. https://doi.org/10.1016/j.molcel.2016.03.031
511 Javaheri A., R. Wysocki, O. Jobin-Robitaille, M. Altaf, J. Cote, *et al.*, 2006 Yeast G1 DNA damage
512 checkpoint regulation by H2A phosphorylation is independent of chromatin remodeling. Proc. Natl.
513 Acad. Sci. 103: 13771–13776. https://doi.org/10.1073/pnas.0511192103
514 Jha S., E. Shibata, and A. Dutta, 2008 Human Rvb1/Tip49 Is Required for the Histone Acetyltransferase
515 Activity of Tip60/NuA4 and for the Downregulation of Phosphorylation on H2AX after DNA Damage.
516 Mol. Cell. Biol. 28: 2690–2700. https://doi.org/10.1128/MCB.01983-07
517 Jiang X., Y. Sun, S. Chen, K. Roy, and B. D. Price, 2006 The FATC domains of PIKK proteins are
518 functionally equivalent and participate in the Tip60-dependent activation of DNA-PKcs and ATM. J.
519 Biol. Chem. 281: 15741–15746. https://doi.org/10.1074/jbc.M513172200
520 Jiang Y., X. Qian, J. Shen, Y. Wang, X. Li, *et al.*, 2015 Local generation of fumarate promotes DNA repair
521 through inhibition of histone H3 demethylation. Nat. Cell Biol. 17: 1158–1168.
522 https://doi.org/10.1038/ncb3209
523 Judes G., K. Rifaï, M. Ngollo, M. Daures, Y. J. Bignon, *et al.*, 2015 A bivalent role of TIP60 histone acetyl
524 transferase in human cancer. Epigenomics.
525 Kalocsay M., N. J. Hiller, and S. Jentsch, 2009 Chromosome-wide Rad51 Spreading and SUMO-H2A.Z-
526 Dependent Chromosome Fixation in Response to a Persistent DNA Double-Strand Break. Mol. Cell 33:
527 335–343. https://doi.org/10.1016/j.molcel.2009.01.016
528 Keogh M., T. A. Mennella, C. Sawa, S. Berthelet, N. J. Krogan, *et al.*, 2006 The Saccharomyces cerevisiae
529 histone H2A variant Htz1 is acetylated by NuA4. Genes Dev. 20: 660–665.
530 https://doi.org/10.1101/gad.1388106
531 Kim M.-Y., E.-J. Ann, J.-Y. Kim, J.-S. Mo, J.-H. Park, *et al.*, 2007 Tip60 Histone Acetyltransferase Acts as a
532 Negative Regulator of Notch1 Signaling by Means of Acetylation. Mol. Cell. Biol.
533 https://doi.org/10.1128/mcb.01515-06
534 Kim H. S., V. Vanoosthuyse, J. Fillingham, A. Roguev, S. Watt, *et al.*, 2009 An acetylated form of histone
535 H2A.Z regulates chromosome architecture in Schizosaccharomyces pombe. Nat. Struct. Mol. Biol. 16:
536 1286–1293. https://doi.org/10.1038/nsmb.1688

537 Kimura A., and M. Horikoshi, 1998 Tip60 acetylates six lysines of a specific class in core histones in vitro.
538 Genes to Cells 3: 789–800. https://doi.org/10.1046/j.1365-2443.1998.00229.x
539 Kobayashi J., A. Kato, Y. Ota, R. Ohba, and K. Komatsu, 2010 Bisbenzamidine derivative, pentamidine
540 represses DNA damage response through inhibition of histone H2A acetylation. Mol. Cancer 9: 1–11.
541 https://doi.org/10.1186/1476-4598-9-34
542 Kobor M. S., S. Venkatasubrahmanyam, M. D. Meneghini, J. W. Gin, J. L. Jennings, *et al.*, 2004 A Protein
543 Complex Containing the Conserved Swi2/Snf2-Related ATPase Swr1p Deposits Histone Variant
544 H2A.Z into Euchromatin. PLoS Biol. 2: 4. https://doi.org/10.1097/GME.0000000000000420
545 Krogan N. J. ., K. Baetz, M. Keogh, N. Datta, C. Sawa, *et al.*, 2004 Regulation of chromosome stability by
546 the histone H2A variant Htz1, the Swr1 chromatin remodeling complex, and the histone
547 acetyltransferase NuA4. Proc. Natl. Acad. Sci. 101: 13513–13518.
548 Kusch T., L. Florens, W. H. MacDonald, S. K. Swanson, R. L. Glaser, *et al.*, 2004 Acetylation by Tip60 is
549 required for selective histone variant exchange at DNA lesions. Science (80-.). 306: 2084–2087.
550 https://doi.org/10.1126/science.1103455
551 La Cruz X. De, S. Lois, S. Sánchez-Molina, and M. A. Martínez-Balbás, 2005 Do protein motifs read the
552 histone code? BioEssays.
553 Lafon A., C. S. Chang, E. M. Scott, S. J. Jacobson, and L. Pillus, 2007 MYST opportunities for growth
554 control: Yeast genes illuminate human cancer gene functions. Oncogene 26: 5373–5384.
555 https://doi.org/10.1038/sj.onc.1210606
556 Langerak P., E. Mejia-Ramirez, O. Limbo, and P. Russell, 2011 Release of Ku and MRN from DNA ends by
557 Mre11 nuclease activity and Ctp1 is required for homologous recombination repair of double-strand
558 breaks. PLoS Genet. 7. https://doi.org/10.1371/journal.pgen.1002271
559 Langerak P., and P. Russell, 2011 Regulatory networks integrating cell cycle control with DNA damage
560 checkpoints and double-strand break repair. Philos. Trans. R. Soc. B Biol. Sci. 366: 3562–3571.
561 https://doi.org/10.1098/rstb.2011.0070
562 Leduc C., P. Claverie, B. Eymin, E. Col, S. Khochbin, *et al.*, 2006 p14ARF promotes RB accumulation
563 through inhibition of its Tip60-dependent acetylation. Oncogene.
564 https://doi.org/10.1038/sj.onc.1209446
565 Leland B. A., A. C. Chen, A. Y. Zhao, R. C. Wharton, and M. C. King, 2018 Rev7 and 53BP1/CRB2
566 prevent RecQ helicase-dependent hyper-resection of DNA double-strand breaks. Elife 7: 1–14.
567 https://doi.org/10.7554/eLife.33402
568 Li L., and Y. Wang, 2017 Cross-talk between the H3K36me3 and H4K16ac histone epigenetic marks in
569 DNA double-strand break repair. J. Biol. Chem. 292: 11951–11959.

570 https://doi.org/10.1074/jbc.M117.788224
571 Manolis K. G., E. R. Nimmo, E. Hartsuiker, A. M. Carr, P. A. Jeggo, *et al.*, 2001 Novel functional
572 requirements for non-homologous DNA end joining in Schizosaccharomyces pombe. EMBO J. 20:
573 210–221. https://doi.org/10.1093/emboj/20.1.210
574 Millar C. B. ., F. Xu, K. Zhang, and M. Grunstein, 2006 Acetylation of H2AZ Lys 14 is associated with
575 genome-wide gene activity in yeast. Genes Dev. 20: 711–722. https://doi.org/10.1101/gad.1395506
576 Minoda A., S. Saitoh, K. Takahashi, and T. Toda, 2005 BAF53/Arp4 Homolog Alp5 in Fission Yeast Is
577 Required for Histone H4 Acetylation, Kinetochore-Spindle Attachment, and Gene Silencing at
578 Centromere. Mol. Biol. Cell 16: 316–327. https://doi.org/10.1091/mbc.E04
579 Miyoshi T., J. Kanoh, and F. Ishikawa, 2009 Fission yeast Ku protein is required for recovery from DNA
580 replication stress. Genes to Cells. https://doi.org/10.1111/j.1365-2443.2009.01337.x
581 Morillo-huesca M., M. Clemente-ruiz, E. Andujar, and F. Prado, 2010 The SWR1 Histone Replacement
582 Complex Causes Genetic Instability and Genome-Wide Transcription Misregulation in the Absence of
583 H2A . Z. PLoS One 5. https://doi.org/10.1371/journal.pone.0012143
584 Morishita T., Y. Tsutsui, H. Iwasaki, and H. Shinagawa, 2003 The Schizosaccharomyces pombe rad60 Gene
585 Is Essential for Repairing Double-Strand DNA Breaks Spontaneously Occurring during Replication and
586 Induced by DNA-Damaging Agents. Mol. Cell. Biol. 23: 3373–3373.
587 https://doi.org/10.1128/mcb.23.9.3373.2003
588 Murr R., J. I. Loizou, Y. G. Yang, C. Cuenin, H. Li, *et al.*, 2005 Histone acetylation by Trrap-Tip60
589 modulates loading of repair proteins and repair of DNA double-strand breaks. Nat. Cell Biol. 8: 91–99.
590 https://doi.org/10.1038/ncb1343
591 Myler L. R., I. F. Gallardo, M. M. Soniat, A. Rajashree, X. B. Gonzalez, *et al.*, 2017 Single-molecule
592 imaging reveals how Mre11-Rad50-Nbs1 initiates DNA break repair. Mol. Cell 67: 891–898.
593 https://doi.org/10.1016/j.molcel.2017.08.002.Single-molecule
594 Naidu S. R., A. J. Lakhter, and E. J. Androphy, 2012 PIASy-mediated Tip60 sumoylation regulates p53-
595 induced autophagy. Cell Cycle 11: 2717–2728. https://doi.org/10.4161/cc.21091
596 Noguchi C., T. Singh, M. A. Ziegler, J. D. Peake, L. Khair, *et al.*, 2019 The NuA4 acetyltransferase and
597 histone H4 acetylation promote replication recovery after topoisomerase I-poisoning. Epigenetics and
598 Chromatin 12: 1–17. https://doi.org/10.1186/s13072-019-0271-z
599 Nugent R. L., A. Johnsson, B. Fleharty, M. Gogol, Y. Xue-Franzén, *et al.*, 2010 Expression profiling of S.
600 pombe acetyltransferase mutants identifies redundant pathways of gene regulation. BMC Genomics 11.
601 https://doi.org/10.1186/1471-2164-11-59
602 Onaka A. T., N. Toyofuku, T. Inoue, A. K. Okita, M. Sagawa, *et al.*, 2016 Rad51 and Rad54 promote

603 noncrossover recombination between centromere repeats on the same chromatid to prevent
604 isochromosome formation. Nucleic Acids Res. 44: 10744–10757. https://doi.org/10.1093/nar/gkw874
605 Ortega-Atienza S., V. C. Wong, Z. DeLoughery, M. W. Luczak, and A. Zhitkovich, 2016 ATM and KAT5
606 safeguard replicating chromatin against formaldehyde damage. Nucleic Acids Res. 44: 198–209.
607 https://doi.org/10.1093/nar/gkv957
608 Osman F., E. A. Fortunato, and S. Subramani, 1996 Double-strand break-induced mitotic intrachromosomal
609 recombination in the fission yeast Schizosaccharomyces pombe. Genetics 142: 341–357.
610 Osman F., M. Adriance, and S. McCready, 2000 The genetic control of spontaneous and UV-induced mitotic
611 intrachromosomal recombination in the fission yeast Schizosaccharomyces pombe. Curr. Genet. 38:
612 113–125. https://doi.org/10.1007/s002940000145
613 Papamichos-Chronakis M., S. Watanabe, O. J. Rando, and C. L. Peterson, 2011 Global regulation of H2A.Z
614 localization by the INO80 chromatin-remodeling enzyme is essential for genome integrity. Cell 144:
615 200–213. https://doi.org/10.1016/j.cell.2010.12.021
616 Pillus L., 2008 MYSTs mark chromatin for chromosomal functions. Curr. Opin. Cell Biol. 20: 326–333.
617 https://doi.org/10.1016/j.ceb.2008.04.009
618 Prudden J., J. S. Evans, S. P. Hussey, B. Deans, P. O'Neill, *et al.*, 2003 Pathway utilization in response to a
619 site-specific DNA double-strand break in fission yeast. EMBO J. https://doi.org/10.1093/emboj/cdg119
620 Renaud-Young M., D. C. Lloyd, K. Chatfield-Reed, I. George, G. Chua, *et al.*, 2015 The NuA4 complex
621 promotes translesion synthesis (TLS)-mediated DNA damage tolerance. Genetics 199: 1065–1076.
622 https://doi.org/10.1534/genetics.115.174490
623 Renaud E., A. Barascu, and F. Rosselli, 2015 Impaired TIP60-mediated H4K16 acetylation accounts for the
624 aberrant chromatin accumulation of 53BP1 and RAP80 in Fanconi anemia pathway-deficient cells.
625 Nucleic Acids Res. 44: 648–656. https://doi.org/10.1093/nar/gkv1019
626 Sabatinos S. A., and S. L. Forsburg, 2010 Molecular genetics of schizosaccharomyces pombe. Methods
627 Enzymol. 470: 759–795. https://doi.org/10.1016/S0076-6879(10)70032-X
628 Sánchez A., and P. Russell, 2015 Ku Stabilizes replication forks in the absence of Brc1. PLoS One.
629 https://doi.org/10.1371/journal.pone.0126598
630 Sapountzi V., I. R. Logan, and C. N. Robson, 2006 Cellular functions of TIP60. Int. J. Biochem. Cell Biol.
631 38: 1496–1509. https://doi.org/10.1016/j.biocel.2006.03.003
632 Scacchetti A., and P. B. Becker, 2021 Variation on a theme: Evolutionary strategies for H2A.Z exchange by
633 SWR1-type remodelers. Curr. Opin. Cell Biol.
634 Schindelin J., I. Arganda-Carreras, E. Frise, V. Kaynig, M. Longair, *et al.*, 2012 Fiji: An open-source
635 platform for biological-image analysis. Nat. Methods.

636 Schuchert P., and J. Kohli, 1988 The ade6-M26 Mutation of Schizosaccharomyces pombe Increases the
637 Frequency of Crossing Over. Genetics 119: 507–515.
638 Semer M., B. Bidon, A. Larnicol, G. Caliskan, P. Catez, *et al.*, 2019 DNA repair complex licenses
639 acetylation of H2A.Z.1 by KAT2A during transcription. Nat. Chem. Biol. 15: 992–1000.
640 https://doi.org/10.1038/s41589-019-0354-y
641 Shao Z., A. J. Davis, K. R. Fattah, S. So, J. Sun, *et al.*, 2012 Persistently bound Ku at DNA ends attenuates
642 DNA end resection and homologous recombination. DNA Repair (Amst). 11: 310–316.
643 https://doi.org/10.1016/j.dnarep.2011.12.007
644 Sharma G. G., S. So, A. Gupta, R. Kumar, C. Cayrou, *et al.*, 2010 MOF and Histone H4 Acetylation at
645 Lysine 16 Are Critical for DNA Damage Response and Double-Strand Break Repair. Mol. Cell. Biol.
646 30: 3582–3595. https://doi.org/10.1128/mcb.01476-09
647 Shastri N., Y. C. Tsai, S. Hile, D. Jordan, B. Powell, *et al.*, 2018 Genome-wide Identification of Structure-
648 Forming Repeats as Principal Sites of Fork Collapse upon ATR Inhibition. Mol. Cell 72: 222-238.e11.
649 https://doi.org/10.1016/j.molcel.2018.08.047
650 Shibata A., P. Jeggo, and M. Löbrich, 2018 The pendulum of the Ku-Ku clock. DNA Repair (Amst). 71:
651 164–171. https://doi.org/10.1016/j.dnarep.2018.08.020
652 Smith E. R., A. Eisen, W. Gu, M. Sattah, A. Pannuti, *et al.*, 1998 ESA1 is a histone acetyltransferase that is
653 essential for growth in yeast. Proc Natl Acad Sci USA 95: 3561–3565.
654 https://doi.org/10.1073/pnas.95.7.3561
655 Soria G., S. E. Polo, and G. Almouzni, 2012 Prime, Repair, Restore: The Active Role of Chromatin in the
656 DNA Damage Response. Mol. Cell 46: 722–734. https://doi.org/10.1016/j.molcel.2012.06.002
657 Stubbe J., and J. W. Kozarich, 1987 Mechanisms of Bleomycin-Induced DNA Degradation. Chem. Rev. 87:
658 1107–1136. https://doi.org/10.1021/cr00081a011
659 Sun Y., X. Jiang, S. Chen, N. Fernandes, and B. D. Price, 2005 A role for the Tip60 histone acetyltransferase
660 in the acetylation and activation of ATM. Proc. Natl. Acad. Sci. U. S. A. 102: 13182–13187.
661 https://doi.org/10.1073/pnas.0504211102
662 Sun Y., X. Jiang, Y. Xu, M. K. Ayrapetov, L. A. Moreau, *et al.*, 2009 Histone H3 methylation links DNA
663 damage detection to activation of the tumour suppressor Tip60. Nat. Cell Biol. 11: 1376–1382.
664 https://doi.org/10.1038/ncb1982
665 Syed A., and J. A. Tainer, 2018 The MRE11–RAD50–NBS1 Complex Conducts the Orchestration of
666 Damage Signaling and Outcomes to Stress in DNA Replication and Repair. Annu. Rev. Biochem. 87:
667 263–294. https://doi.org/10.1146/annurev-biochem-062917-012415
668 Sykes S. M., H. S. Mellert, M. A. Holbert, K. Li, R. Marmorstein, *et al.*, 2006 Acetylation of the p53 DNA-

669 Binding Domain Regulates Apoptosis Induction. Mol. Cell 24: 841–851.
670 https://doi.org/10.1016/j.molcel.2006.11.026
671 Tang Y., J. Luo, W. Zhang, and W. Gu, 2006 Tip60-Dependent Acetylation of p53 Modulates the Decision
672 between Cell-Cycle Arrest and Apoptosis. Mol. Cell 24: 827–839.
673 https://doi.org/10.1016/j.molcel.2006.11.021
674 Tang J., N. W. Cho, G. Cui, E. M. Manion, N. M. Shanbhag, *et al.*, 2013 Acetylation limits 53BP1
675 association with damaged chromatin to promote homologous recombination. Nat. Struct. Mol. Biol. 20:
676 317–325. https://doi.org/10.1038/nsmb.2499
677 Teixeira-Silva A., A. Ait Saada, J. Hardy, I. Iraqui, M. C. Nocente, *et al.*, 2017 The end-joining factor Ku
678 acts in the end-resection of double strand break-free arrested replication forks. Nat. Commun. 8.
679 https://doi.org/10.1038/s41467-017-02144-5
680 Thomas T., and A. K. Voss, 2007 The diverse biological roles of MYST histone acetyltransferase family
681 proteins. Cell Cycle.
682 Tomita K., A. Matsuura, T. Caspari, A. M. Carr, Y. Akamatsu, *et al.*, 2003 Competition between the Rad50
683 Complex and the Ku Heterodimer Reveals a Role for Exol in Processing Double-Strand Break. Mol.
684 Cell. Biol. 23: 5186–5197. https://doi.org/10.1128/MCB.23.15.5186
685 Utley R. T., and J. Côté, 2003 The MYST family of histone acetyltransferases. Curr. Top. Microbiol.
686 Immunol.
687 Van H. T., and M. A. Santos, 2018 Histone modifications and the DNA double-strand break response. Cell
688 Cycle.
689 Voss A. K., and T. Thomas, 2009 MYST family histone acetyltransferases take center stage in stem cells and
690 development. BioEssays.
691 Walworth N. C., and R. Bernards, 1996 rad-Dependent Response of the chk1-Encoded Protein Kinase at the
692 DNA Damage Checkpoint. Science (80-.). 271: 353–356.
693 Wan S., H. Capasso, and N. C. Walworth, 1999 The topoisomerase I poison camptothecin generates a Chk1-
694 dependent DNA damage checkpoint signal in fission yeast. Yeast 15: 821–828.
695 https://doi.org/10.1002/(SICI)1097-0061(199907)15:10A<821::AID-YEA422>3.0.CO;2-#
696 Wang H., and X. Xu, 2017 Microhomology-mediated end joining: New players join the team. Cell Biosci. 7:
697 4–9. https://doi.org/10.1186/s13578-017-0136-8
698 Xhemalce B., and T. Kouzarides, 2010 A chromodomain switch mediated by histone H3 Lys 4 acetylation
699 regulates heterochromatin assembly. Genes Dev. 24: 647–652. https://doi.org/10.1101/gad.1881710
700 Xu Y., Y. Sun, X. Jiang, M. K. Ayrapetov, P. Moskwa, *et al.*, 2010 The p400 ATPase regulates nucleosome
701 stability and chromatin ubiquitination during DNA repair. J. Cell Biol. 191: 31–43.

702 https://doi.org/10.1083/jcb.201001160
703 Xu Y., M. K. Ayrapetov, C. Xu, O. Gursoy-Yuzugullu, Y. Hu, *et al.*, 2012 Histone H2A.Z Controls a
704 Critical Chromatin Remodeling Step Required for DNA Double-Strand Break Repair. Mol. Cell 48:
705 723–733. https://doi.org/10.1016/j.molcel.2012.09.026
706 Yan Z., C. Xue, S. Kumar, J. B. Crickard, Y. Yu, *et al.*, 2019 Rad52 Restrains Resection at DNA Double-
707 Strand Break Ends in Yeast. Mol. Cell 76: 699-711.e6. https://doi.org/10.1016/j.molcel.2019.08.017
708 Yu Y., J. Y. Ren, J. M. Zhang, F. Suo, X. F. Fang, *et al.*, 2013 A proteome-wide visual screen identifies
709 fission yeast proteins localizing to DNA double-strand breaks. DNA Repair (Amst). 12: 433–443.
710 https://doi.org/10.1016/j.dnarep.2013.04.001
711 Zhou B. O., S. S. Wang, L. X. Xu, F. L. Meng, Y. J. Xuan, *et al.*, 2010 SWR1 Complex Poises
712 Heterochromatin Boundaries for Antisilencing Activity Propagation. Mol. Cell. Biol. 30: 2391–2400.
713 https://doi.org/10.1128/MCB.01106-09
714 Zhu Z., W. H. Chung, E. Y. Shim, S. E. Lee, and G. Ira, 2008 Sgs1 Helicase and Two Nucleases Dna2 and
715 Exo1 Resect DNA Double-Strand Break Ends. Cell 134: 981–994.
716 https://doi.org/10.1016/j.cell.2008.08.037
717 Zlatanova J., and A. Thakar, 2008 H2A.Z: View from the Top. Structure 16: 166–179.
718 https://doi.org/10.1016/j.str.2007.12.008
719

720 **Figure Legends**

721 **Figure 1. The *mst1-L344S* allele affects DSB repair. A.** *mst1-L344S* are sensitive to bleomycin. Cells were
722 grown in YES media overnight at 25ºC then 5X serial dilutions were spotted onto YES plates or YES plates
723 containing bleomycin. Plates were incubated at 25ºC and photographed after 4 days. 1 unit of bleomycin = 1
724 mg (by potency). **B.** An assay to test chromosomal instability from (Osman *et al.* 1996). Two non-functional
725 *ade6* alleles flank the functional *ura4*$^{+}$ gene. *the ade6-L469* has a mutation at the C terminus while the *ade6-*
726 *M26* allele has a mutation at the N-terminus (indicated by the vertical lines). Several recombination outcomes
727 are possible and are described in results and methods. **C.** Cells were grown in YES media overnight at 25ºC
728 then 5X serial dilutions were spotted onto YES (*HO* repressed) or PMG without thiamine (*HO* induced). Plates
729 were incubated at 25ºC and photographed after 5 days. **D**. Percent of deletion, conversion and complex
730 rearrangements after double strand break induction in WT and *mst1-L344S* using the assay in **B**. The bold line
731 in each box represents median and the filled circles represent outliers. Asterisks indicate that recombination
732 percentage is significantly different than WT ($p<0.05$, Mann-Whitney Test). **E**. Chromatin
733 immunoprecipitation assay to test recruitment of Rad52-YFP and Mst1-V5 to a single DNA double strand
734 break in WT and *clr4*Δ. Using a construct from Du, Nakamura, and Russell 2006 with one single double strand
735 break can be made with the *HO* endonuclease and protein interaction with chromatin can be monitored at 0.2
736 and 2KB from the break. Following break induction, time points were taken at 0, 22, 24 and 26 hours. qPCR
737 was done with primers provided in Du, Nakamura, and Russell 2006. Asterisks represent fold enrichment is
738 significantly different than that in WT ($p<0.1$, Student's t-test). **F.** *clr4*Δ had lower percentage of cells with
739 Rad52 foci after single DSB induction. **Top:** Percentage of cells with Rad52 foci using a construct from Du,
740 Nakamura, and Russell 2006 with one single double strand break can be made with the *HO* endonuclease.
741 Following break induction, cultures were taken at 0, 22, 24 and 26 hours as in Figure 1E and cells were imaged
742 under microscope. Asterisks represent fold enrichment is significantly different than that in WT ($p<0.05$,
743 Student's t-test). **Bottom:** Examples of WT and *clr4*Δ cells with Rad52 foci upon DSB induction.

744 **Figure 2. The *mst1-L344S* mutant affects recruitment of repair proteins at 25ºC A. Top:** Percentage of
745 cells with RPA (Rad11) and Rad52 foci in WT, *mst1-L344S*, *pht1-4KR*, *pht1*Δ, *ku70*Δ and *ku70*Δ *mst1-L344S.*
746 The bold line in each box represents median and the filled circles represent outliers. Asterisks represent
747 percentage of cells with foci is significantly different than that in WT (*: $p<0.05$, **: $p<0.01$, Mann-Whitney
748 Test) **Bottom:** Examples of WT and *mst1-L344S* cells with Rad11 and Rad52 foci. Scale bar is 10µm. Rad11-
749 CFP is colored magenta for visibility. **B. Top:** Percentage of cells with Rad54 foci in WT and *mst1-L344S,*
750 *pku70*Δ *and pku70*Δ *mst1-L344S.* The bold line in each box represents median and the filled circles represent
751 outliers. **Bottom:** Examples of WT and *mst1-L344S* cells with Rad54 foci under phleomycin treatment. Scale
752 bar is 10µm. **C. Top:** Percentage of cells with colocalized Rad52-CFP and HO-induced mCherry foci over

753 240 minutes. **Bottom:** Representatives of WT and *mst1-L344S* cells with Rad52-CFP and HO-induced
754 mCherry foci over time. Rad52-CFP is colored green for visibility. **D.** Percentage of cells with mCherry-LacI
755 signal over 240 minutes. Image was taken every 8 min in wild-type and *mst1-L344S*, and every 48 min in other
756 mutants.

757 **Figure 3. *mst1-L344S* mutants are sensitive to the DSB-inducing agent bleomycin.** *pku70*Δ, *exo1*Δ **A.** and
758 *pht1-4KR* **B.** growth in bleomycin. Cells were grown in YES media overnight at 25ºC then 5X serial dilutions
759 were spotted onto YES plates or YES plates containing bleomycin. Plates were incubated at 25ºC and
760 photographed after 4 days. 1 unit of bleomycin = 1 mg (by potency)

761 **Figure 4. Mst1 affects DNA lesion repair but does not affect checkpoint activation. A. Left:** Percentage
762 of cells with RPA (Rad11) and Rad52 foci in WT and *mst1-L344S* after CPT and MMS treatments. The bold
763 line in each box represents median and the filled circles represent outliers. **Right:** examples of WT and *mst1-*
764 *L344S* cells with RPA and Rad52 foci after drug treatment. Scale bar is 10µm. Rad11-CFP is colored magenta
765 for visibility. **B**. Phosphorylation of Chk1-HA is not affected in *mst1-L344S* after treatment of cells with three
766 types of DNA damaging agents at 32°C. cells were treated for 4 hours with 0.01% MMS, 15mM HU or 40µM
767 CPT and the and the Chk1-HA phosphorylation shift band was detected by Western blotting with 12CA5 anti-
768 HA antibody. **C**. H2A phosphorylation dynamics are not affected in *mst1-L344S* when cells are treated with
769 40µM CPT. Western Blot with an anti-phosphorylated H2A antibody showing that phosphorylation of H2A
770 peaks 4 hours after treatment with drug then the signal is down regulated 4 hours post drug removal. *hta1-*
771 *S129A:* control non-phosphorylatable form of H2A; α-PCNA: control antibody.

772 **Figure 5. Model for the function of Mst1 in DSB repair.** Mst1 facilitates HR by promoting long-range
773 resection and inhibiting Ku70-associated mechanism that inhibits HR. Such function is accomplished by
774 acetylating H2A.Z and thus promoting the turnover of H2A.Z at the DSB. Therefore, the histone variant can
775 no longer block the break site. The removal of H2A.Z allows Exo1 to access the break and thus promotes
776 downstream recombination-mediated repair.

777 **Supplementary Figure S1. *mst1-L344S* mutants are sensitive to Bleomycin analog Phleomycin.** Cells
778 were grown in YES media overnight at 25ºC then 5X serial dilutions were spotted onto YES plate or YES
779 plates containing Phleomycin. Plates were incubated at 25ºC and photographed after 4 days.

780 **Supplementary Figure S2**. **Examples of cells with RPA (Rad11), Rad52, and Rad54 foci after treatment**
781 **with phleomycin at 25ºC**. **A.** Rad11-CFP and Rad52-YFP foci in *pku70Δ* and *pku70Δ mst1-L344S*. **B.** Rad11-
782 CFP and Rad52-YFP foci in *pht1-4KR* and *pht1Δ*. **C.** Rad54-GFP foci in *pku70Δ* and *pku70Δ mst1-L344S.*

783 **Supplementary Figure S3. *pku70*Δ does not affect cell length at septation in *mst1-L344S* at 25ºC.** Length
784 at septation at 25ºC of WT, *mst1-L344S*, *pku70*Δ, and *pku70*Δ *mst1-L334S* cells. The bold line in each box
785 represents median and the filled circles represent outliers.

786 **Supplementary Figure S4. *mst1-L344S* interacts genetically with genes in the checkpoint pathways.** Cells
787 were grown in YES media overnight at 32ºC then 5X serial dilutions were spotted onto YES plate or YES
788 plates containing the indicated drugs. Plates were incubated at 32ºC and photographed after 4 days.
789 **Supplementary Table S1.** Median, first and third quantiles of cells with Rad11, Rad52 or Rad54 percentage
790 shown in Figure 2A and 2B.
791 **Supplementary Table S2.** Strains used in this study.
792

Figure 1. The *mst1-L344S* allele affects DSB repair.

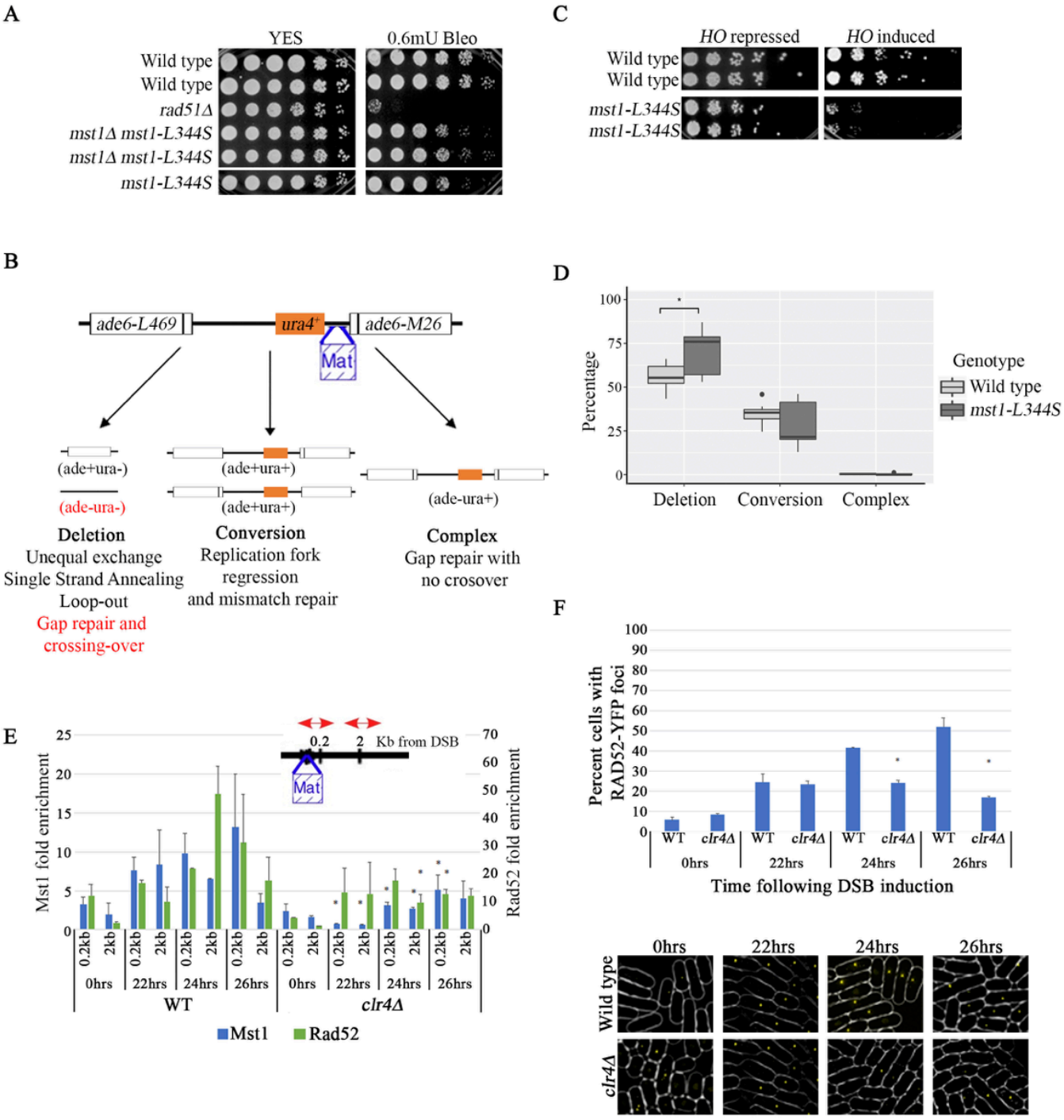

793

Figure 2. The *mst1-L344S* mutant affects recruitment of repair proteins.

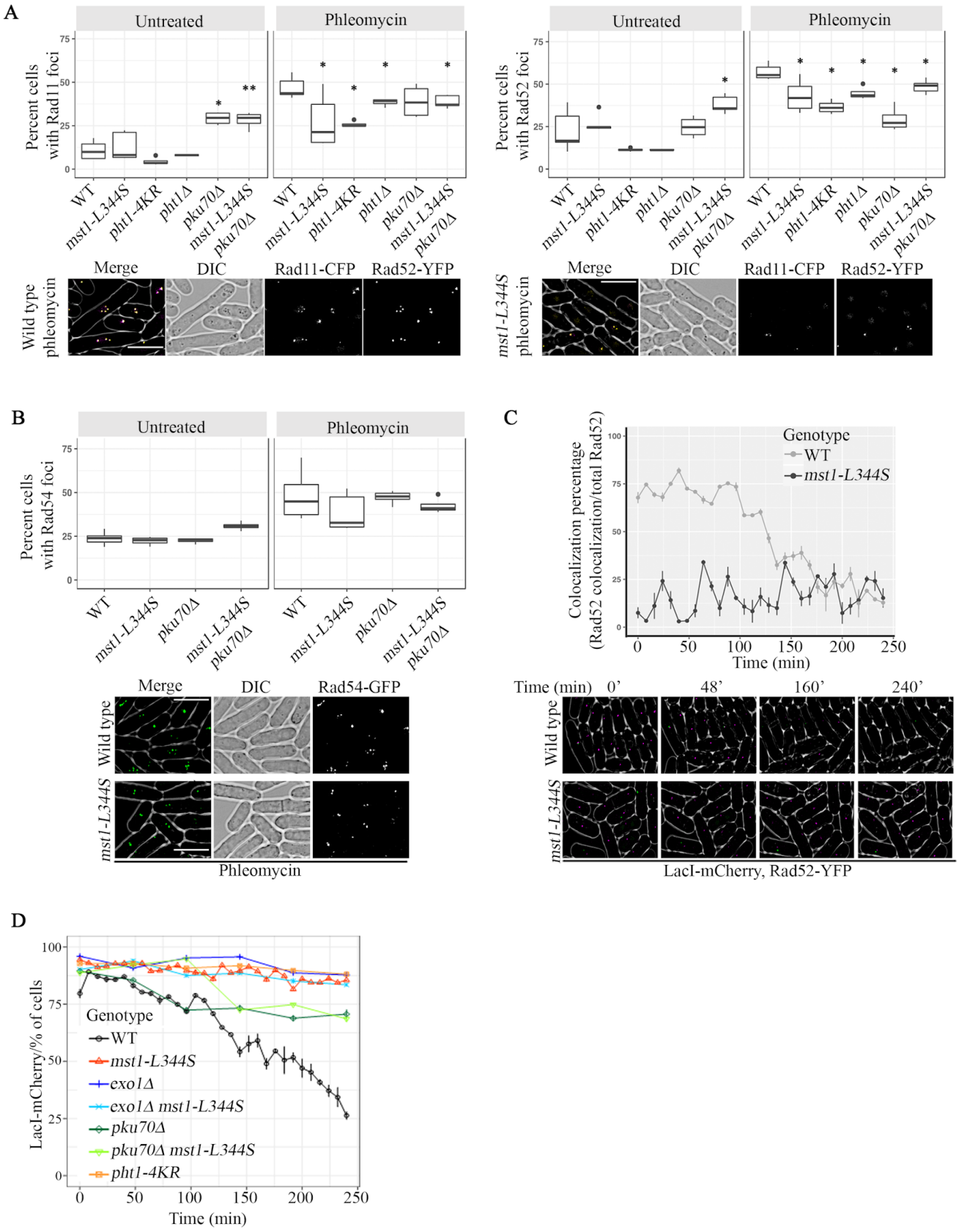

794

Figure 3. *mst1-L344S* mutants are sensitive to the DSB-inducing agent bleomycin.

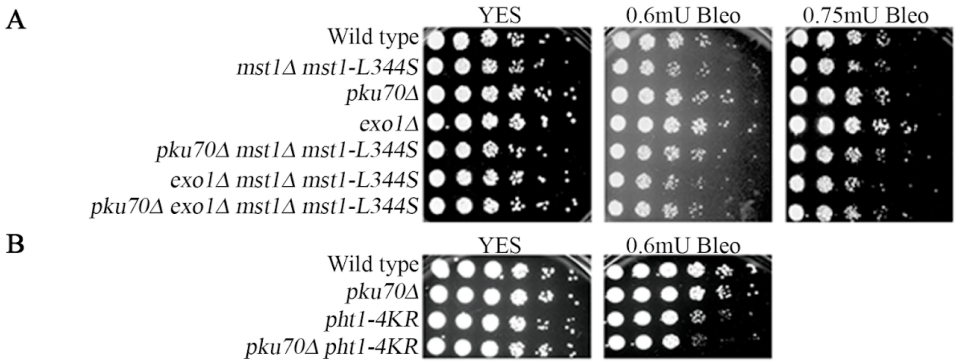

795

Figure 4. Mst1 affects DNA lesion repair but does not affect checkpoint activation.

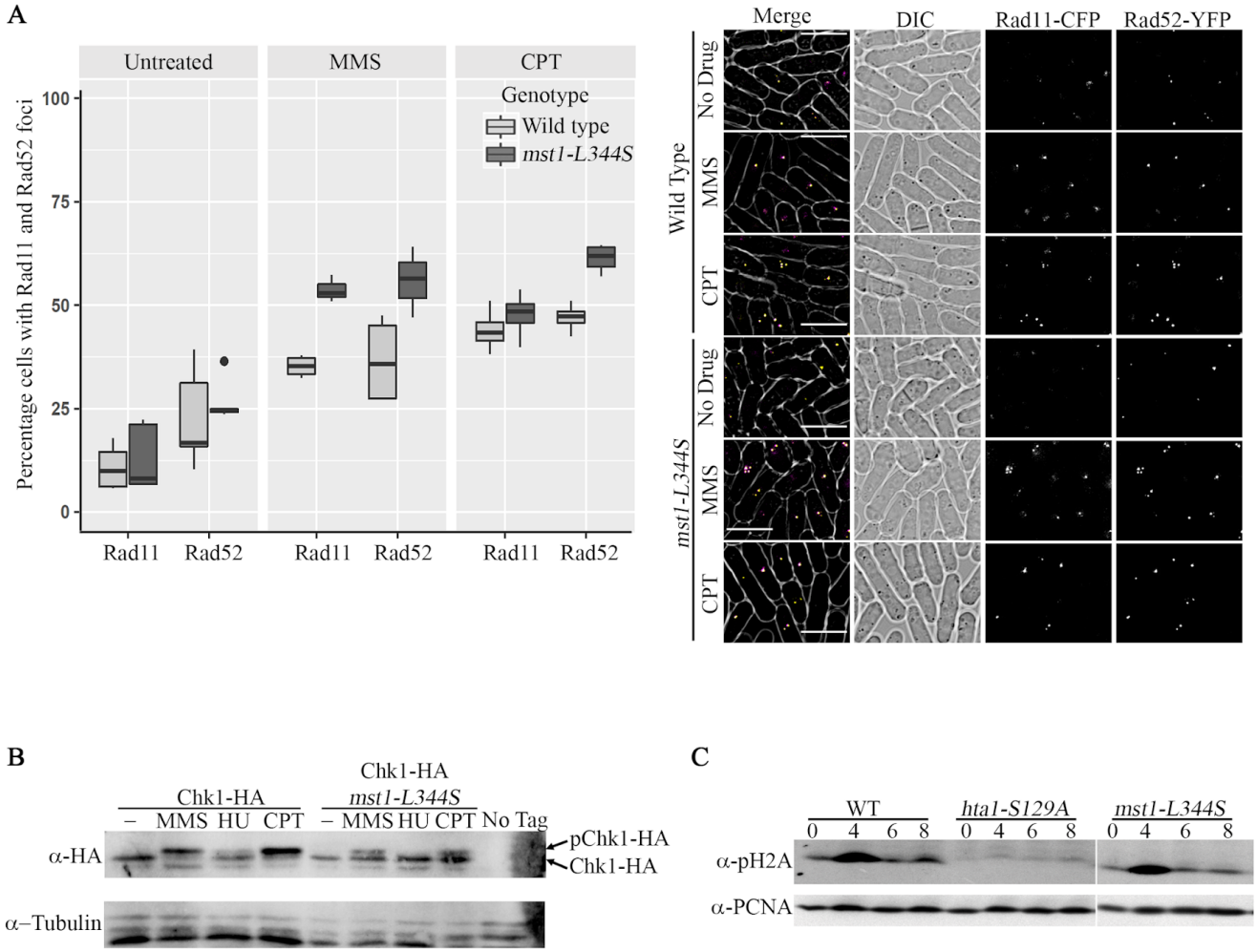

796

Figure 5. Model for the function of Mst1

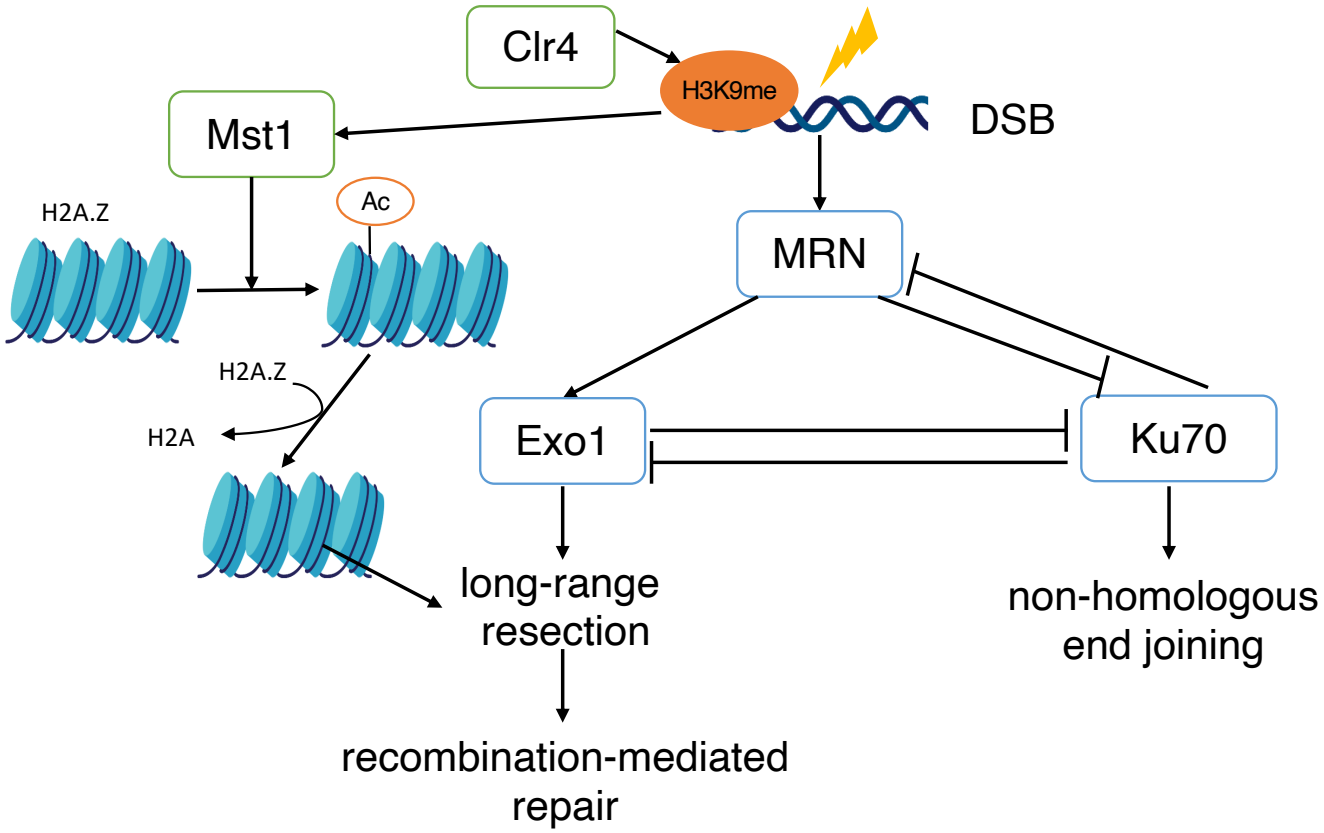

797

Supplementary Figure S1. The *mst1-L344S* mutants are sensitive to the bleomycin analog phelomycin.

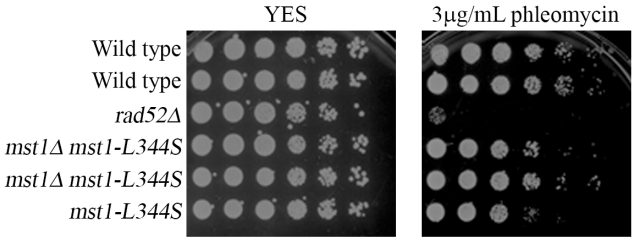

798

Supplementary Figure S2. Examples of cell with RPA (Rad11), Rad52, and Rad54 foci after treatement with phleomycin.

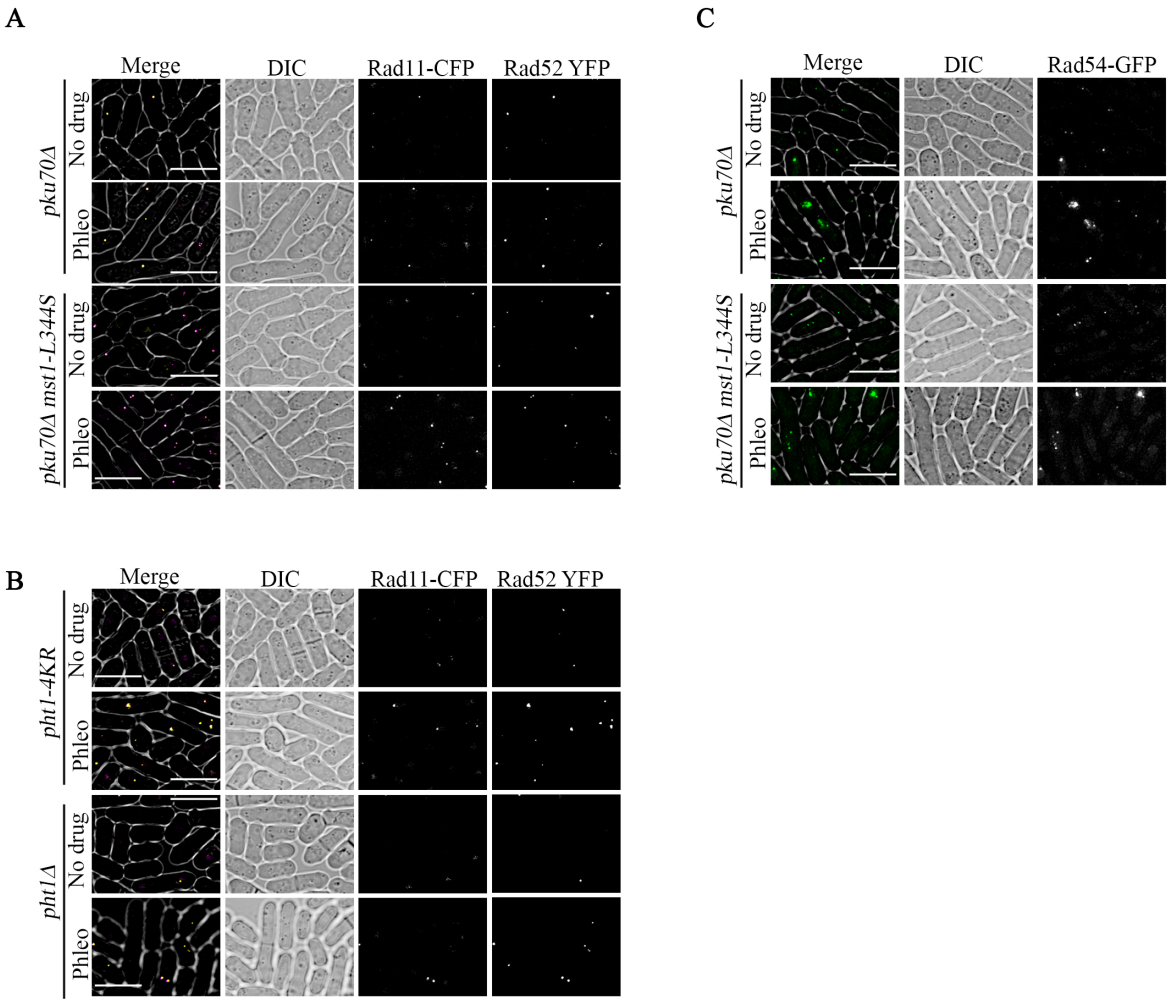

Supplementary Figure S3. ***pku70Δ*** does not affect cell length at septation in ***mst1-L344S*** at 25°C.

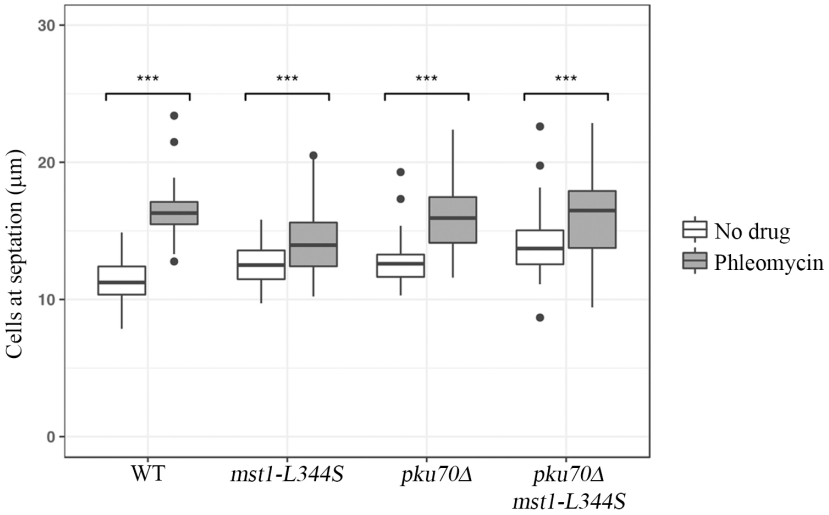

800

Supplementary Figure S4. ***mst1-L344S*** interacts genetically with genes in the checkpoint pathways.

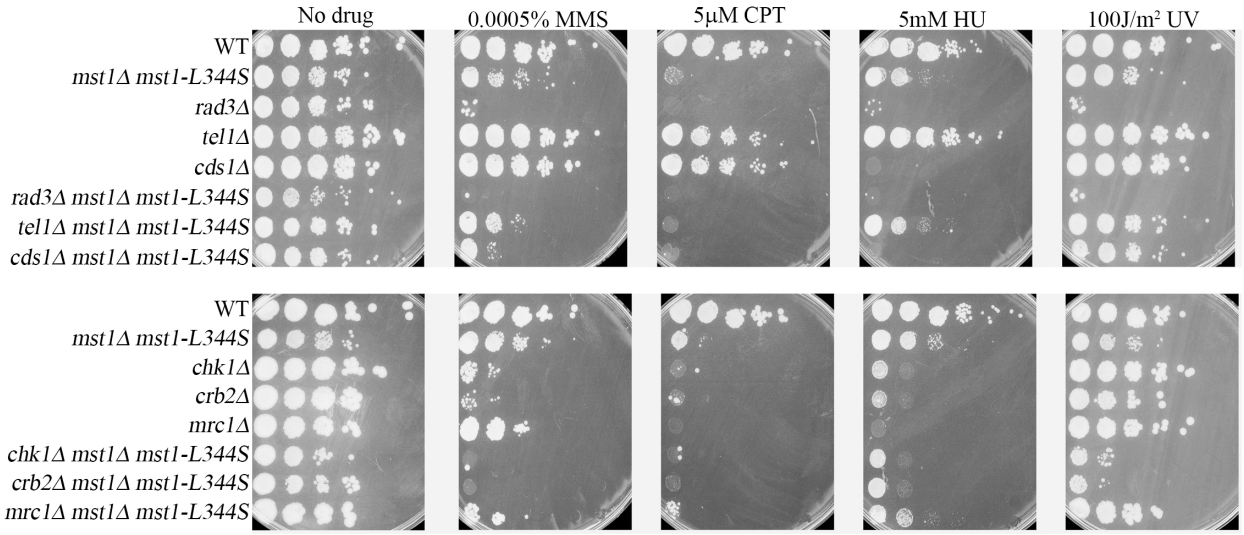

801

Supplementary Table S1. Median, first and third quartiles of cells with Rad11-CFP, Rad52-YFP and Rad54-GFP foci percentages.

	Rad11		
	Median	1st Quantile	3rd Quantile
WT Untreated	9.9	6.1	14.51
WT Phleomycin	43.72	42.98	50.7
mst1-L344S Untreated	8.14	6.76	21.15
mst1-L344S Phleomycin	21.3	15.38	37.29
pht1-4KR Untreated	3.58	3.25	4.78
pht1-4KR Phleomycin	24.96	24.76	25.95
*pht1*Δ Untreated	7.99	7.7	8.36
*pht1*Δ Phleomycin	39.2	37.75	39.86
*pku70*Δ Untreated	29.48	26.4	32.27
*pku70*Δ Phleomycin	38.31	30.99	46.27
*pku70*Δ *mst1-L344S* Untreated	29.5	26.38	31.32
*pku70*Δ *mst1-L344S* Phleomycin	37.08	36.62	42.3

	Rad52		
	Median	1st Quantile	3rd Quantile
WT Untreated	16.67	15.85	31.17
WT Phleomycin	55.4	53.77	60
mst1-L344S Untreated	24.73	24.12	24.89
mst1-L344S Phleomycin	41.85	35.76	24.89
pht1-4KR Untreated	11.26	10.98	11.63
pht1-4KR Phleomycin	36.05	33.84	38.7
*pht1*Δ Untreated	11.11	11.11	11.51
*pht1*Δ Phleomycin	43.42	42.53	45.59
*pku70*Δ Untreated	24.7	20.28	29.16
*pku70*Δ Phleomycin	27.19	24.71	31.83
*pku70*Δ *mst1-L344S* Untreated	35.75	35.2	42.32
*pku70*Δ *mst1-L344S* Phleomycin	49.09	46.02	50.4

	Rad54		
	Median	1st Quantile	3rd Quantile
WT Untreated	23.91	21.72	25.22
WT Phleomycin	44.91	37.34	54.55
mst1-L344S Untreated	22.74	21.18	23.85
mst1-L344S Phleomycin	32.7	30.28	47.48
*pku70*Δ Untreated	23.04	22.06	23.47
*pku70*Δ Phleomycin	47.78	46.09	49.55
*pku70*Δ *mst1-L344S* Untreated	30.74	29.99	31.6
*pku70*Δ *mst1-L344S* Phleomycin	40.97	40.04	43.37

802

803 **Supplementary Table S2.** Strains used in this study.
804

Strain	Genotype	Source
FY254	*h- can1-1 leu1-32 ade6-M210 ura4-D18*	Our stock
FY255	*h+ can1-1 leu1-32 ade6-M210 ura4-D18*	Our stock
FY527	*h- his3-D1 ade6-M216 ura4-D18 leu1-32*	Our stock
FY528	*h+ his3-D1 ade6-M210 ura4-D18 leu1-32*	Our stock
FY421	*h- ade6-704 leu1-32 ura4-D18 Δchk1::ura4*	Our stock
FY4743	*h- rad11-Cerulean::hphMX rad22-YFP-natMX leu1-32 ade6-M210 ura4-D18*	Our stock
FY8927	*h90 mst1-L344S-5FLAG:hphMX6 rad11-Cerulean::hphMX rad22-YFP-natMX leu1-32 ura4-D18*	This study
FY1106	*h+ Δrad3::ura4+ ura4-D18 leu1-32 ade6-M210*	Our stock
FY1204	*h+ Δrhp51::ura4+ ade6-704 leu1-32 ura4-D18*	Our stock
FY1353	*h+ leu1-32 ura4-D18 his3-D1 ade6-M210 pku70::kanr*	Our stock
FY2396	*h- Δmst1::ura4+ leu1::nmt-mst1L-S leu1+ ura4-D18 ade6-M210*	Our stock
FY2449	*h+ Δmst1::kanMX6 leu1::nmt-mst1L-S-leu1+ ura4-D18 ade6-M210*	Our stock
FY2450	*h- Δmst1::kanMX6 leu1::nmt-mst1L-S-leu1+ ura4-D18 ade6-M210*	Our stock
FY2504	*h- Δrhp9::ura4+ (=crb2) mst1::kanMX6 leu1::nmt-mst1L-S-leu1+ ura4-D18 leu1-32 ade6-M21?*	This study
FY2643	*h- Δchk1::ura4+ Δmst1::kanMX6 leu1::nmt-mst1L-S-leu1+ ura4-D18 ade6-M210 or 704*	Our stock
FY2725	*h- Δpku70::kanr Δmst1::ura4+ leu1::nmt-mst1L-S leu1+ ura4-D18 ade6-M210*	Our stock
FY2726	*h- Δpku70::kanr Δmst1::ura4+ leu1::nmt-mst1L-S leu1+ ura4-D18 ade6-M210*	Our stock
FY3135	*h- ade6-M210 leu1-32 ura4-D18 hip1::ura4+*	Simon Whitehall
FY3151	*h- Δmrc1::ura4+ ura4-D18 leu1-32 his7-366*	Our stock
FY3439	*h- ura4-D18 leu1-32 ade6-M216 his3-D1 Δrhp9::ura4+ (=crb2)*	Our stock
FY3562	*h+ Δmst1::kanMX6 leu1::nmt-mst1L-S-leu1+ ade6-M210 ura4-D18 Δhip1::ura4+*	Our stock
FY3857	*h+ Δrhp51::ura4+ Δmst1::kanMX6 leu1::nmt-mst1L-S leu1+ura4-D18 leu1-32*	This study
FY3884	*h- exo1::ura4 ura4-D18*	Mathew O'Connell
FY4713	*h- Δmst1::kanMX6 Δmrc1::ura4+ leu1::nmt-mst1L-S-leu1+ ura4-D18 ade6-M210 leu1-32*	This study
FY5304	*h+ Δmst1::kanMX6 leu1::nmt-mst1L-S-leu1+ exo1::ura4+ ura4-D18 leu1-32*	This study
FY5311	*h+ pht1-4KtoR-3HA-KanMX6 ura4-D18 leu1-32 ade6-M216 his3-D1*	Michael Keogh
FY6024	*h+ mst1-L344S-5FLAG:hphMX6 leu1-32 ura4-D18*	Eishi Noguchi
FY6229	*h- leu1-32 ura4-D18 ade6-M26 int::pUC8/ura4+/MATa/ade6-L469 his3-D1 ade6-M216*	Our stock
FY6632	*h- pku70::kanr his3-D1 ura4-D18 leu1-32 ade6-M216*	Our stock
FY8929	*h- mst1-L344S-5FLAG:hphMX6 leu1-32 ura4-D18 ade6-M26 int::pUC8/ura4+/MATa/ade6-L469 his3-D1 ade6-M216*	This study
FY9153	*h+ pht1::ura4 rad11-Cerulean::hphMX rad22-YFP-natMX leu1-32 ade6-M210 ura4-D18*	Our stock
FY9154	*h+ pht1-4KtoR-3HA-KanMX6 rad11-Cerulean::hphMX rad22-YFP-natMX ura4-D18 leu1-32 ade6-M216/210 his3-D1?*	This study

FY9338	*h- mst1-L344S-5FLAG:hphMX6 pku70::kanr rad11-Cerulean::hphMX rad22-YFP-natMX leu1-32 ura4-D18 his3-D1? ade6-M210*	This study
FY9352	*h- pku70::kanr rad11-Cerulean::hphMX rad22-YFP-natMX leu1-32 ura4-D18 his3-D1? ade6-M210*	This study
FY8989	*h- rad54-GFP:hphMX6*	Takuro Nakagawa
FY9023	*h- mst1-L344S-5FLAG:hphMX6 rad54-GFP:hphMX6 leu1-32? ura4-D18?*	This study
FY9340	*h- pku70::kanr rad54-GFP:hphMX6 leu1-32? his3-D1? ade6-M210?*	This study
FY9353	*h- mst1-L344S-5FLAG:hphMX6 pku70::kanr rad54-GFP:hphMX6 leu1-32? his3-D1? ade6-M210?*	This study
FY7479	*h- arg3::HOsite-natMX ars1::p41nmt1-HO(his3+) lys1-131::pdis1-mCherry-lacI(lys1+) erg7ter::lacO(ura4+) rad52-tandemCFP::kanMX leu1-32 his3-D1 ura4-294*	Li-Lin Du
FY8992	*h- mst1-L344S-5FLAG:hphMX6 arg3::HOsite-natMX ars1::p41nmt1-HO(his3+) lys1-131::pdis1-mCherry-lacI(lys1+) erg7ter::lacO(ura4+) rad52-tandemCFP::kanMX leu1-32 his3-D1 ura4-294/D18?*	This study
FY4620	*h- chk1HA(ep) cds1-myc::KanMX ade6-M216 ura4-D18 leu1-32*	Our stock
FY9495	*h+ exo1Δ::hph arg3::HOsite-natMX ars1::p41nmt1-HO(his3+) lys1-131::pdis1-mCherry-lacI(lys1+) erg7ter::lacO(ura4+) rad52-tandemCFP::kanMX leu1-32 his3-D1 ura4-294*	This study
FY9499	*h- pku70::kanr arg3::HOsite-natMX ars1::p41nmt1-HO(his3+) lys1-131::pdis1-mCherry-lacI(lys1+) erg7ter::lacO(ura4+) rad52-tandemCFP::kanMX leu1-32 his3-D1 ura4-294/D18 ade6-M210?*	This study
FY9502	*h- pht1-4KtoR-3HA-KanMX6 arg3::HOsite-natMX ars1::p41nmt1-HO(his3+) lys1-131::pdis1-mCherry-lacI(lys1+) erg7ter::lacO(ura4+) rad52-tandemCFP::kanMX leu1-32 his3-D1 ura4-294/D18?*	This study
FY9514	*h+ exo1Δ::hph mst1-L344S-5FLAG:hphMX6 arg3::HOsite-natMX ars1::p41nmt1-HO(his3+) lys1-131::pdis1-mCherry-lacI(lys1+) erg7ter::lacO(ura4+) rad52-tandemCFP::kanMX leu1-32 his3-D1 ura4-294*	This study
FY9542	*h- pku70::kanr mst1-L344S-5FLAG:hphMX6 arg3::HOsite-natMX ars1::p41nmt1-HO(his3+) lys1-131::pdis1-mCherry-lacI(lys1+) erg7ter::lacO(ura4+) rad52-tandemCFP::kanMX leu1-32 his3-D1 ura4-294/D18 ade6-M210?*	This study
FY5083	*h- Δmst1::kanMX6 leu1::nmt-mst1L-S-leu1+ chk1HA(ep) cds1-myc::KanMX ura4-D18 ade6-M210/216?*	This study
FY3397	*h- leu1-32 ura4-D18 ade6-M210 his3-D1 hta1-S129A:ura4+ hta2-S128A:his3+*	Takuro Nakagawa
FY5548	*h- ura4-D18 leu1-32 his3-D1 ade6-M210 mst1::[mst1-V5 leu1+] rad22-YFP::hphMX arg3::HOsite(KanMX4) ars1::nmt41-HOendonuclease:ampR:his3+:ars1*	Our stock
FY9561	*h- clr4::kanMX6-Bioneer mst1::[mst1-V5 leu1+] rad22-YFP::hphMX arg3::HOsite(KanMX4) ars1::nmt41-HOendonuclease:ampR:his3+:ars1his3-D1 ura4-D18 leu1-32 ade6-M210*	This study